Constitutive and ghrelin-dependent GHSR1a activation impairs $Ca_V2.1$ and $Ca_V2.2$ currents in hypothalamic neurons

E.J. López Soto[1], F. Agosti[1], A. Cabral[2], E.R. Mustafa[1], V. Martínez Damonte[1], M.A. Gandini[3], S. Rodríguez[1], D. Castrogiovanni[1,2], R. Felix[3], M. Perelló[2] and J. Raingo[1].

[1]Laboratory of Electrophysiology, [2]Laboratory of Neurophysiology; Multidisciplinary Institute of Cell Biology (CONICET/CICPBA), La Plata City, Buenos Aires, Argentina. [3]Department of Cell Biology; Center for Research and Advanced Studies of the National Polytechnic Institute, Mexico City, Mexico.

jraingo@imbice.gov.ar

Abstract

The growth hormone secretagogue receptor type 1a (GHSR1a) has the highest known constitutive activity of any G protein coupled receptor (GPCR). GHSR1a mediates the action of the hormone ghrelin and its activation increases transcriptional and electrical activity in hypothalamic neurons. Although GHSR1a is present at GABAergic presynaptic terminals, its effect on neurotransmitter release remains unclear. The activities of the voltage gated calcium channels, $Ca_V2.1$ and $Ca_V2.2$, which mediate neurotransmitter release at presynaptic terminals, are modulated by many GPCRs. Here, we show that both constitutive and agonist-dependent GHSR1a activity elicit a strong impairment of $Ca_V2.1$ and $Ca_V2.2$ currents in rat and mouse hypothalamic neurons and in a heterologous expression system. Constitutive GHSR1a activity reduces Ca_V2 currents by a $G_{i/o}$-dependent mechanism that involves persistent reduction in channel density at the plasma membrane, whereas ghrelin-dependent GHSR1a inhibition is reversible and involves altered Ca_V2 gating via a G_q-dependent pathway. Thus, GHSR1a differentially inhibits Ca_V2 channels by $G_{i/o}$- or G_q-protein pathways depending on its mode of activation. Moreover, we present evidence suggesting that GHSR1a-mediated inhibition of Ca_V2 attenuates GABA release in hypothalamic neurons, a mechanism that could contribute to neuronal activation through the disinhibition of postsynaptic neurons.

Teaser: Constitutive and ligand-dependent GHSR1a activity attenuates Ca_V2 current and hypothalamic GABA release through distinct mechanisms and signaling pathways.

Introduction

GHSR1a is a G-protein coupled receptor (GPCR) highly expressed in the hypothalamus (Zigman et al., 2006). Ghrelin, the natural GHSR1a agonist, is a potent growth hormone secretagogue and it is the only known orexigenic peptide hormone (Nakazato et al., 2001). Ghrelin-induced GHSR1a activation in soma and dendrites regulates gene transcription and increases electrical activity in neurons (Nakazato et al., 2001; Cowley et al., 2003; Diano et al., 2006; Andrews et al., 2008; Shi et al., 2013; Ribeiro et al., 2014). In addition, GHSR1a activation modulates neurotransmitter release at presynaptic terminals (Cowley et al., 2003; Cui et al., 2011; Yang et al., 2011). The modulation of presynaptic voltage-gated calcium channels ($Ca_V2.1$ and $Ca_V2.2$) is a well-established mechanism by which GPCRs regulate neurotransmitter release at central synapses (Catterall and Few, 2008; Zamponi and Currie, 2013). However, the potential role of GHSR1a regulating Ca_V2 channels has not been tested.

GHSR1a displays two uncommon features: a high constitutive activity and multiple signaling cascades that greatly increase the complexity of this receptor's function. Constitutive GHSR1a activity is about 50% of the maximum activity triggered by saturating concentrations of ghrelin (Holst et al., 2003), and it is proposed to contribute to the physiological roles of the ghrelin/GHSR1a system (Petersen et al., 2009). However, the mechanisms by which constitutive GHSR1a activity regulates neuronal activity in hypothalamic neurons remain poorly understood. On the other hand, despite it is well known that GHSR1a activates G_q proteins (Howard et al., 1996; Holst et al., 2003), recent reports indicate that other G proteins, such as $G_{i/o}$ and $G_{12/13}$, and also G protein independent pathways, such as β-arrestin recruitment, can mediate GHSR1a actions (Bennett et al., 2009; Evron et al., 2014).

Here, we used a combination of genetic and pharmacological manipulations of GHSR1a activity to show that both constitutive and ghrelin-dependent GHSR1a activities inhibit $Ca_V2.1$ and $Ca_V2.2$. We found fundamental differences in the mechanisms of Ca_V2 inhibition by constitutive and agonist dependent modes of GHSR1a activation; including the signaling cascades involved and the fact that constitutive activity reduces membrane channel protein levels. Moreover, we found that GHSR1a impairs GABA release in hypothalamic neurons. Based on our data we propose that this GHSR1a-depedent regulation of Ca_V2 could modify presynaptic function in the hypothalamus, particularly under fasting, when GHSR1a expression is increased.

Materials and Methods

Animals

Sprague-Dawley rats and GHSR-eGFP reporter mice (STOCK Tg(Ghsr-EGFP)KZ65Gsat/Mmucd, #030942-UCD, Mouse Mutant Regional Resource Center, University of California, United States) were bred at the animal facility of the IMBICE. We housed the animals in a 12 hour light/dark cycle in a climate controlled room (22 °C) with *ad libitum* access to water and food, except when indicated. We carried out this study in strict accordance with the recommendations of the Guide for the Care and Use of Laboratory Animals of the National Research Council, United States, and all efforts were made to minimize suffering. All experimentation received approval from the Institutional Animal Care and Use Committee of the IMBICE.

Rat neuronal primary cultures

Neuronal cultures were obtained from Sprague-Dawley rats at embryonic day 16-17. The procedure protocol was similar to the one described in (Raingo et al., 2012). Briefly, we anesthetized pregnant rats with chloral hydrate (500 mg/kg) and removed the embryos. We exposed the embryo brains and placed them on the dorsal face to remove the hypothalamus with forceps. We placed the blocks of tissue in sterile Hank's solution, and, after two washes, we dissociated the cells at 37 °C for 20 min with Hank´s solution containing trypsin 0.25 mg/ml (cat#L2700-100, Microvet, Buenos Aires, Argentina) and deoxyribonuclease I from bovine pancreas 0.28 mg/ml (cat#D5025, Sigma Aldrich, Missouri, United States), then we added 300 µl of Fetal Bovine Serum (FBS, cat#1650-01, Internegocios, Buenos Aires, Argentina) to stop the enzyme digestion. We mechanically dissociated the cells using several glass pipettes with consecutive smaller tips diameters. We plated 70,000 cells on 12 mm diameter glass coverslips previously treated with poly-L-lysine (cat#P8920, Sigma Aldrich) and laid over 24 well plates. We incubated the cells at

37 °C in a 95% air and 5% CO_2 atmosphere with Dulbecco Modified Eagle Medium (DMEM, cat# P3030, Microvet)/F12 1:1 medium supplemented with 10% FBS, 0.25% glucose, 2 mM glutamine (cat#21051-016, GIBCO, United States), 3.3 µg/ml insulin (Nordisk Pharm Ind, Inc, North Carolina, United States), 5 U/ml penicillin G sodium salt (Richet, Buenos Aires, Argentina), 5 µg/ml streptomycin (Richet), 40 µg/ml gentamicin sulfate salt (Richet) and 1 % vitamin solution (cat#L2112-100, Microvet). On the fourth day in culture, we replaced half of the incubation medium with fresh medium containing cytosine β-D-arabinofuranoside (AraC, cat# C1768, Sigma Aldrich) to reach a final concentration of 5 µM.

Mouse neuronal primary cultures

We used embryonic day 16-17 GHSR-eGFP reporter mice. The procedure protocol was similar to the one described above. The culture conditions were the same except for the addition of B27 supplement (1:50) (cat#17504-044, GIBCO) to the incubation medium.

Rat neuron transfections

At the 6^{th} day in culture, we transfected rat neurons with GHSR1a-YFP, GHSR1a-A204E-YFP or eGFP containing plasmids using calcium phosphate technique (Jiang and Chen, 2006). We performed patch clamp recordings on green fluorescent and non-green neurons after 48 h in culture.

HEK 293T cells culture and transfection

For patch clamp experiments, we co-transfected 80% confluent HEK 293T cells with GHSR1a or GHSR1a-A204E and $Ca_V2.1$ (GENBANK#AY714490) or $Ca_V2.2$ (GENBANK#AF055477) and the calcium channel auxiliary subunits $Ca_V\alpha_2\delta_1$ (GENBANK#AF286488) and $Ca_V\beta_3$ (GENBANK#M88751) or $Ca_V\beta_{2a}$ (GENBANK#M80545)

in a 1:1:1:1 molar ratio using Lipofectamine 2000 (Invitrogen). Also, for GHSR1a constitutive activity studies, we decreased the amount of GHSR1a cDNA transfected as indicated in the results section. For some experiments, we co-transfected empty pcDNA3.1(+), the C-terminal G protein coupled receptor kinase 2 (MAS-GRK2-ct) (Kammermeier and Ikeda, 1999; Raingo et al., 2007) or a $G\alpha_q$ dominant negative mutant ($G\alpha_q$-Q209L/D277N, cat#GNA0Q000C0, Missouri S&T cDNA Resource Center, Missouri, United States). For imaging experiments, we replaced $Ca_V2.1$ and $Ca_V2.2$ by these proteins tagged with GFP. GHSR1a and GHSR1a-A204E clones were provided by Dr. Jacky Marie (Universités Montpellier I & II, France), Untagged Ca_V clones used for this study were a gift from Dr. Diane Lipscombe (Brown University, United States) and $Ca_V2.1$-GFP was provided by Erika S. Piedras-Renteria (Loyola University Chicago, United States).

F-ghrelin binding

We transfected HEK 293T cells with 0.15 or 0.6 µg of GHSR1a or 0.6 µg of empty pcDNA3.1+ plasmid as a control. We incubated the cells with 0.4 mM fluorescein-ghrelin (F-ghrelin (McGirr et al., 2011)) in binding buffer (50 mM HEPES, pH 7.4, 5 mM $MgCl_2$, 1 mM $CaCl_2$, 0.2% BSA, passed through a 0.45 µm filter). After 30 min, we washed the cells with PBS, we fixed them with formaldehyde 4%, and covered them with mounting media. We observed the cells with an Eclipse 50i Nikon microscope with a 500 nm filter. We took photomicrographs with a DS-Ri1 Nikon camera and analyzed the photomicrographs with the ImageJ 1.48v software.

Electrophysiology

We recorded ionic currents with an Axopatch 200 amplifier (Molecular Devices, California, United States). We sampled data at 20 kHz and filtered at 10 kHz (-3 dB) using

pClamp8.2 software. We used recording electrodes with resistances between 2-4 MΩ when filled with internal solution. We admitted series resistances less than 6 MΩ and compensated 80% with a 10 μs lag time. We subtracted current leak on-line using a P/-4 protocol (except for the measure of evoked and miniature postsynaptic currents). We performed all recordings at room temperature.

i- Sodium and barium currents of primary neuronal cultures. We patch-clamped 7-10 day *in vitro* rat and mouse cultured neurons in voltage-clamp whole-cell mode. Internal pipette solution contained (in mM): 134 CsCl, 10 EGTA, 1 EDTA, 10 HEPES, 4 MgATP (pH 7.2 with CsOH). We measured sodium currents with high sodium external solution containing (in mM): 135 NaCl, 4.7 KCl, 1.2 $MgCl_2$, 2.5 $CaCl_2$, 10 HEPES, 10 glucose (pH 7.4 with NaOH). To measure Ca_V currents, we replaced the external solution by a high barium solution with the neurons clamped at negative potentials. High barium solution contained (in mM): 10 $BaCl_2$, 110 choline chloride, 20 tetraethyl-ammonium chloride, 1 $MgCl_2$, 10 HEPES, 10 glucose and 0.001 tetrodotoxin (TTX, cat# T8024, Sigma Aldrich) (pH 7.4 with CsOH). We held neurons at -80 mV and applied test pulses to 0 mV for 20 ms every 10 s. Current-voltage relationship (IV) protocol: we applied increasing square test pulses of 20 ms of duration ranging from -60 to +50 mV every 5 s (Raingo et al., 2007).

ii- Postsynaptic currents of primary neuronal cultures: We patch-clamped 10-17 day *in vitro* mouse neurons. Internal pipette solution contained (in mM): 115 Cs-methanesulfonate, 10 CsCl, 5 NaCl, 10 HEPES, 20 tetraethylammonium chloride, 4 Mg-ATP, 0.3 NaGTP, 0.6 EGTA and 10 lidocaine N-ethyl bromide (pH 7.2 with CsOH). The external solution used was the high sodium solution described above, containing 10 μM 6-cyano-7-nitroquinoxaline-2,3-dione (Alomone Labs, Jerusalem, Israel) in order to isolate inhibitory postsynaptic currents (IPSCs). To elicit evoked responses, we delivered electrical stimulation through parallel platinum electrodes (duration, 1 ms; amplitude, 20

mA) while neurons were held at -80 mV. We added 1 µM TTX in order to record miniature IPSCs (mIPSCs).

iii- Calcium currents of transiently transfected HEK 293T cells. We performed whole-cell patch clamp recordings on transfected HEK 293T cells. The internal solution was the same described for sodium and barium currents. External solution contained (in mM): 2 $CaCl_2$, 140 choline chloride, 1 $MgCl_2$, 10 HEPES (pH 7.4 with CsOH). Test pulses protocol: we applied square pulses from -100 mV to 10 mV for 15 or 20 ms every 10 s. Pre-pulse protocol: we applied a pre-pulse of 15 ms at +80 mV 12.5 ms before the test pulse to remove effectively all voltage-dependent inhibition of Ca_V (Raingo et al., 2007; Lopez Soto and Raingo, 2012). This protocol has no effect on both $Ca_V2.1$ and $Ca_V2.2$ control current densities ($Ca_V2.1$ currents without pre-pulse = -54.60 ± 16.97 pA/pF vs. with pre-pulse = -54.27 ± 16.92 pA/pF, n=13, $p>0.05$; and $Ca_V2.2$ currents without pre-pulse = -46.28 ± 14.53 pA/pF vs. with pre-pulse = -45.38 ± 14.23 pA/pF, n=8, $p>0.05$; Paired t-tests). Current-voltage relationship (IV) protocol: we applied increasing square test pulses of 20 ms of duration ranging from -60 to +50 mV every 5 s (Raingo et al., 2007).

Imaging

We transfected HEK 293T cells with $Ca_V2.1$-GFP (gifted by Dr. Erika Piedras Renteria, Cao et al., 2004) or $Ca_V2.2$-GFP, both obtained by sub-cloning in pEGFP-C1 vector, its auxiliary subunits ($Ca_V\alpha2\delta1$ and $Ca_V\beta3$) and GHSR1a or GHSR1a-A204E as previously described. 48 h or 24 h after transfection for $Ca_V2.1$-GFP or $Ca_V2.2$-GFP respectively, we replaced the culture medium by 1 ml of 1 µg/ml membrane marker solution (CellMaskTM Orange Plasma membrane Stain, cat# c10045, Molecular probes, California, United States) and kept the cells at 37 ºC for 1 min. Then, we washed three times with PBS. Finally, we removed almost all the PBS volume and placed a clean coverslip over the cell

layer. We obtained fluorescence photomicrographs with an Eclipse 50i optical fluorescence microscope, equipped with B2A and G2A filters and with a Nikon DS-Ri1 camera. We performed the analysis on photomicrographs with FIJI free software, using the CellMask red signal to mark out the plasma membrane and quantify green fluorescence intensity in both the internal area (excluding plasma membrane) and the total area of each cell as integrated density. We calculated the fluorescence intensity corresponding to the membrane (membrane fluorescence) as the difference between the fluorescence corresponding to the total (total fluorescence) and the internal area. Then we calculated the percentage of $Ca_V2.1$-GFP or $Ca_V2.2$-GFP membrane fluorescence as = (membrane fluorescence/total fluorescence) * 100; for each cell.

Western-blots

We used Lipofectamine Plus reagent (Invitrogen) to transfect HEK 293T cells with $Ca_V2.1$ or $Ca_V2.2$, the Ca_V channel auxiliary $Ca_V\alpha_2\delta_1$ and $Ca_V\beta_3$ subunits, as well as the GHSR1a and the GHSR1a-A204E or the pCDNA3.1 empty vector. We extracted membrane protein using a membrane protein extraction kit (cat# K268-50, BioVision) as reported elsewhere (Gandini et al., 2014). For each condition, we used six 100 mm culture plates of HEK 293T cells expressing Ca_V channels. We determined cytosolic and plasma membrane protein concentration using the bicinchoninic acid assay. Briefly, 40/50 µg of protein samples were boiled for 5 min in protein-loading buffer (1.7% SDS, 0.1 M 2-mercaptoethanol, 5% glycerol, 58 mM Tris–Cl, and 0.002% bromophenol blue; pH 6.8), resolved in 7% SDS-polyacrylamide gels and transferred to nitrocellulose membranes (Immobilon, Millipore). After blocking with 5% nonfat dry milk in Tris-buffered saline Tween 20 (TBST; 100 mM Tris–Cl, 0.9% (w/v) NaCl, and 0.2% Tween 20; pH 7.5), we incubated membranes overnight with primary antibodies: anti-$Ca_V2.1$ (1: 300 in TBST 2.5% milk, Alomone Laboratories cat# ACC-001), anti-$Ca_V2.2$ (1:200 in TBST, Calbiochem cat#

681505), anti-Cadherin (1:200 in TBST, Zymed cat# 71-7100), anti-AKT (1:15000 in TBST, Santa Cruz Biotechnology, Texas, United States, cat# sc-81434) and anti-Hsp90 (1:2000 in TBST, Cell Signaling cat# 4875). Then, we washed membranes and incubated them with horseradish peroxidase (HRP)- conjugated secondary antibodies (Anti-rabbit HRP, 1:5000 in TBST Jackson Inmunolabs cat# 111-035-003; Anti-mouse HRP; 1:5000 in TBST Jackson Inmunolabs cat# 115-035-033) diluted in TBST-5% nonfat dry milk. For semi-quantitative analysis, we normalized Ca_V channels signal to the Cadherin signal. We used the MacBiophotonics ImageJ program (National Institutes of Health) for densitometry analysis.

Ex-vivo determination of [3H]-GABA release in Arcuate nucleus (ARC)

We euthanized *ad-libitum* fed and 48 h fasted mice by live decapitation. We extracted brains, placed them briefly in cold PBS, and sectioned them into 1-mm coronal slices by using a stainless steel mouse brain matrix. We excised small punches of tissue corresponding to the known location of the ARC, as compared to the mouse brain atlas (Paxinos and Franklin, 2001), using a 15-g needle. We incubated the ARC micro-dissections on Krebs-Ringer Bicarbonate Buffer (KRBB) saturated with 95% O_2 and 5% CO_2 for 10 min at 37 °C. Then, we incubated with [3H]-GABA (367cpm/ml, with a specific activity of 92.1 Ci/mmol) (Perkin Elmer) in KRBB for 20 min to fill synaptic vesicles with the tracer and we performed two washes with KRBB. After that, we incubated ARC micro-dissections for 10 min with fresh KRBB containing 56 mM KCl. Finally, we collected the medium, mixed it with 150 µl of scintillator (Ecolite) and measured the radioactivity in a β-counter (Tracor Analytic).

qRT-PCR analysis

We euthanized *ad-libitum* fed and 48 h fasted mice by live decapitation. We extracted brains, placed them briefly in cold diethylpyrocarbonate-PBS, and excised small punches of tissue corresponding to the ARC, as explained above. We then performed qRT-PCR analysis as described in (Chuang et al., 2011a). Briefly, we isolated total RNA from these punches using RNA STAT-60 (Tel-Test Inc.). We treated the RNA with RNase-free DNase (Roche) and reverse-transcribed into cDNA with SuperScript II reagents (Invitrogen). We performed a quantitative PCR using an Applied Biosystems 7900HT Sequence Detection System and SYBR Green chemistry (Applied Biosystems). Primers were mGHSR-QF1, 5'-ACCGTGATGGTATGGGTGTCG-3', and mGHSR-QR1, 5'-CACAGTGAGGCAGAAGACCG-3`, they amplified a product within exon 2 of the ghsr gene. We confirmed these results by a second set of specific primers, one of which is located in exon 1 of the ghsr gene (mGHSR-QF3 [5'-ATCTCCAGTGCCAGGCACTGCT-3']) and the other of which is located in exon 2 (mGHSR-GR3 [5'-AATGGGCGCGAGCAGCAGGAA-3']) of the ghsr gene. The mRNA relative levels were expressed relative to the housekeeping gene 36B4 and calculated by the comparative threshold cycle (ΔΔCt) method (Kurrasch et al., 2004). The data are presented as a percentage of levels observed in wild-type ARC punches.

Drugs

We used ghrelin esterified with n-octanoic acid (cat# PI-G-03, Global Peptide, Colorado, United States); a GHSR1a inverse agonist, [D-Arg1,D-Phe5,D-Trp7,9,Leu11]-Substance P (SPA, cat# sc-361166, Santa Cruz Biotechnology); the inhibitor of G_s protein, cholera toxin (ChTx, cat# C8052, Sigma Aldrich); a specific inhibitor of $G_{i/o}$ protein, pertussis toxin (PTx, cat# P7208, Sigma Aldrich); the $Ca_V2.1$ blocker, ω-agatoxin-IVA (cat# 4256-s, Peptides International, Kentucky, United states); the $Ca_V2.2$ blocker, ω-conotoxin-GVIA (cat# C-300, Alomone lab, Israel).

Statistics

We analyzed and plotted the data using the OriginPro 8 (OriginLab Corp., Massachusetts, United States) and GraphPad Prism 5 (GraphPad Software Inc., California, United States). We examined the normal distribution of data by Kolmogorov-Smirnov test. Based on the normality test results we established statistical significance ($p < 0.05$) by one- or two-sample t-test (normal distributed data) or Mann-Whitney test (no normal distributed data), and multiple comparison ANOVA with Dunnett's or Tukey's post-test (normal distributed data) or, non-parametric Kruskal-Wallis test with Dunns post-test (no normal distributed data). The specific statistical test used is detailed in each case. We expressed data as mean ± standard error with the number of observations in brackets.

Results

Constitutive and ghrelin-dependent GHSR1a activities differentially inhibit Ca_V2 currents in a heterologous expression system

We first examined the effect of GHSR1a and GHSR1a-A204E, a mutant lacking constitutive activity (Pantel et al., 2006), on cloned $Ca_V2.1$ and $Ca_V2.2$ channels. We co-expressed GHSR1a and Ca_V2 in a 1:1 molar ratio (0.6 µg of receptor cDNA per transfection) and measured calcium currents in HEK 293T cells. Calcium currents were significantly smaller in cells co-expressing GHSR1a and Ca_V2, as compared to those expressing Ca_V2 alone. By contrast, Ca_V2 currents in cells co-expressing GHSR1a-A204E were not different from control recordings. We next tested if agonist-independent GHSR1a-induced inhibition of Ca_V2 varies with GHSR1a expression levels. Thus, we measured Ca_V2 currents in cells transfected with $Ca_V2.1$ or $Ca_V2.2$ channels and different amounts of GHSR1a plasmid and found that Ca_V2 current amplitudes were inversely

proportional to GHSR1a cDNA amount per transfection (Figure 1A). Moreover, we found that F-ghrelin binding positively correlated with the level of GHSR1a cDNA used in the transfection (Figure 1B). Then we measured basal Ca_V2 currents in cells expressing GHSR1a with or without pre-incubation with the GHSR1a inverse agonist, substance P analog (SPA, 1 μM), for 16 h and we found no significant difference with currents recorded in cells co-expressing GHSR1a-A204E (Figure 1C). To assess ghrelin-dependent GHSR1a action on Ca_V2 currents, we used GHSR1a-A204E, which lacks constitutive activity but is prone to activation by agonist binding. Application of a saturating dose of ghrelin (0.5 μM, (Pantel et al., 2006)) inhibited both Ca_V2 subtypes, but it was more effective on $Ca_V2.2$ as compared to $Ca_V2.1$ currents (44.5 ± 6.9 % n = 8 vs. 15.4 ± 3.9 %, n = 5, respectively at 0.6 μg of receptor cDNA; t-test, p = 0.01). Moreover, to test if ghrelin-mediated effect was independent on GHSR1a expression levels and A204E mutation we applied ghrelin in cells transfected with 0.15, 0.3 and 0.6 μg of GHSR1a or 0.6 μg of GHSR1a-A204 containing cDNA per well and $Ca_V2.1$ or $Ca_V2.2$ and its auxiliary subunits. When 0.6 μg of GHSR1a cDNA were used for transfections we tested the effect of ghrelin only in cell that showed a measurable amount of current. We found that ghrelin-evoked GHSR1a activation inhibits $Ca_V2.1$ and $Ca_V2.2$ independently of A204E mutation and at the same extent in all the GHSR1a cDNA amounts tested (Figure 1D).

We obtained two more sets of evidence toward two differential inhibitory mechanisms of constitutive and ghrelin-evoked GHSR1a's effects on Ca_V2 currents: ghrelin application inhibits calcium currents in HEK 293T cells expressing $Ca_V2.1$ or $Ca_V2.2$ and GHSR1a in a 1:1 molar ratio pre-incubated with SPA, despite the fact that constitutive GHSR1a activity is blocked (Figure 2A). In addition, we found that acute application of SPA was unable to remove Ca_V2 inhibition by constitutive GHSR1a activity (Figure 2B).

Thus, our data show that constitutive GHSR1a activity inhibits $Ca_V2.1$ and $Ca_V2.2$ channels by a long term mechanism that depends on GHSR1a expression levels. By contrast, ghrelin-dependent GHSR1a activity is more effective to inhibit $Ca_V2.2$ as compared to $Ca_V2.1$ currents and this inhibition is fast and independent of GHSR1a expression levels.

Two different signaling cascades are involved in Ca_V2 inhibition by constitutive and ghrelin-dependent GHSR1a activities

Next, we tested the hypothesis that differential mechanisms mediate the inhibition of Ca_V2 channels by constitutive and ghrelin-dependent GHSR1a activities. We examined the signaling pathways engaged by GHSR1a that result in Ca_V2 inhibition. We first assessed the effectiveness of ghrelin-induced activation of GHSR1a-A204E on $Ca_V2.2$ channels expressed in HEK 293T cells. Neither the G_s protein inhibitor Cholera toxin (ChTx, 500 ng/ml) nor the $G_{i/o}$ protein inhibitor Pertussis toxin (PTx, 500 ng/ml) affected ghrelin-mediated inhibition of $Ca_V2.2$ currents (Figure 3A). We therefore used a mutant form of $G\alpha_q$ (G_qDN) that acts as a dominant negative interfering with G_q-dependent signaling (Yu and Simon, 1998; Lauckner et al., 2005) and we found that G_qDN occluded the inhibitory actions of ghrelin on $Ca_V2.2$ (Figure 3A).

Then, we tested if the same G protein signaling pathway also mediates the inhibitory actions of constitutive GHSR1a activity on $Ca_V2.2$ currents independently of ghrelin. We found that neither G_qDN nor pre-treatment with ChTx affect $Ca_V2.2$ current amplitude in cells expressing GHSR1a. By contrast, $Ca_V2.2$ currents in cells co-expressing GHSR1a pre-treated with PTx were not different from the currents recorded in cells co-expressing GHSR1a-A204E (Figure 3B). This result suggests that GHSR1a inhibits $Ca_V2.2$ channels through $G_{i/o}$ protein activation by an agonist-independent mechanism. Next, we incubated cells expressing the wild type receptor, GHSR1a, with PTx, and then determine

whether the agonist still modulates channel activity. We found that ghrelin inhibits the currents in this experimental condition suggesting that the agonist-mediated and constitutive activity of GHSR1a modulates Ca_V2 channels by two independent pathways (Figure 3C).

GPCR-mediated inhibition of $Ca_V2.2$ is mediated for at least 3 different G proteins and the downstream mechanisms can be voltage-sensitive or voltage-insensitive (Zamponi and Currie, 2013). The most common form of $G_{i/o}$-dependent inhibition of $Ca_V2.2$ channels involves direct binding of $G_{\beta\gamma}$ to the channel, and it is relieved by strong depolarizing pre-pulses (voltage-sensitive) (Ikeda, 1996; Raingo et al., 2007; Lipscombe et al., 2013). On the other hand, several G_α protein subtypes (G_q, $G_{i/o}$ and G_s) activate voltage-insensitive forms of Ca_V2 inhibition (Kammermeier and Ikeda, 1999; Kammermeier et al., 2000; Zamponi and Currie, 2013; Agosti et al., 2014). We found that inhibition of $Ca_V2.2$ channels by ghrelin-induced activation of GHSR1a-A204E is not relieved by +80 mV pre-pulses, consistent with a purely voltage-independent mechanism and a G_q-mediated pathway (Figure 3D). However, it is known that G_q-mediated inhibition of $Ca_V2.2$ channels turns into a voltage sensitive inhibition by substituting the $Ca_V\beta_3$ for a membrane bound form, $Ca_V\beta_{2a}$ (Keum et al., 2014). Thus, we assayed ghrelin-mediated inhibition of $Ca_V2.2$ with $Ca_V\beta_{2a}$ as auxiliary subunit. We found that ghrelin-mediated inhibition of $Ca_V2.2$ was not only reduced, as compared to the inhibition of $Ca_V2.2$ channels formed by $Ca_V\beta_3$, but also completely reversed by +80 mV pre-pulses (Figure 3C). Moreover, we co-expressed the MAS-GRK2-ct peptide to sequester $G_{\beta\gamma}$ (Kammermeier and Ikeda, 1999; Raingo et al., 2007) and found that this maneuver fully occluded the inhibitory actions of ghrelin-GHSR1a-A204E on $Ca_V2.2$ channels co-expressed with either $Ca_V\beta_{2a}$ or $Ca_V\beta_3$. Taken together, our results demonstrate that ghrelin-mediated GHSR1a activation inhibits $Ca_V2.2$ currents by a mechanism that involves G_q, $G_{\beta\gamma}$ subunits of G proteins and whose voltage

dependency relies on the $Ca_V\beta$ subtype. On the other hand, we found that inhibition of $Ca_V2.2$ by constitutive GHSR1a activity is unaltered by strong pre-pulses to +80 mV, $Ca_V\beta$ subtype or $G_{\beta\gamma}$ sequestration (Figure 3E). Thus, our results suggest that agonist-dependent and agonist-independent forms of $Ca_V2.2$ inhibition by GHSR1a signal through different pathways.

Ca_V2 inhibition by constitutive GHSR1a activity is associated with a reduced channel density at the plasma membrane

Based in our results showing that the GHSR1a inverse agonist, SPA, requires long pre-incubation periods in order to occlude constitutive inhibition of Ca_V2 by GHSR1a, we decided to test if surface Ca_V2 density was affected by constitutive GHSR1a activity. First, we monitored the presence of Ca_V2 channels in the plasma membrane, using $Ca_V2.1$ and $Ca_V2.2$ channels tagged with GFP ($Ca_V2.1$-GFP and $Ca_V2.2$-GFP) that we have confirmed are functional in our experimental conditions ($Ca_V2.1$-GFP current -47.0 ± 14.5 pA/pF, n = 9; $Ca_V2.2$-GFP current = -51.8 ± 12.3 pA/pF, n = 5). In order to identify the surface location of the GFP fluorescence signal, we used the red fluorescent membrane marker CellMaskTM (Cogger et al., 2010). We found that $Ca_V2.1$-GFP and $Ca_V2.2$-GFP -associated fluorescence signal was significantly lower in cells co-expressing GHSR1a, as compared to those co-expressing GHSR1a-A204E or those co-expressing GHSR1a and pre-incubated with SPA or PTx (Figure 4A). Next, we used western blots in order to confirm that the $Ca_V2.1$ and $Ca_V2.2$ membrane protein level is decreased when cells co-express GHSR1a. We used HEK 293T cells transfected with $Ca_V2.1$ or $Ca_V2.2$, as well as GHSR1a, GHSR1a-A204E or the pcDNA3.1 empty vector. By using cadherin as a plasma membrane marker, and AKT and Hsp90 as cytoplasmic protein markers, we found that $Ca_V2.1$ and $Ca_V2.2$ protein quantity decreased in the plasma membrane protein fraction

when cells co-express GHSR1a, while GHSR1a-A204E co-expression failed to affect the amount of $Ca_V2.1$ and $Ca_V2.2$ plasma membrane protein (Figure 4B). In summary, our data suggest that constitutive GHSR1a activity reduces surface expression of $Ca_V2.1$ and $Ca_V2.2$ channels by a $G_{i/o}$-dependent mechanism.

Constitutive and ghrelin-dependent GHSR1a activities inhibit native N- and P/Q-type currents

In order to test the effect of GHSR1a activities on calcium channels in native conditions, we used hypothalamic primary neuronal cultures of GHSR-eGFP reporter mice in which GHSR1a expressing neurons are identifiable by green fluorescent signal (Mani et al., 2014). We first compared Ca_V currents recorded in GHSR1a-positive (GHSR1a+) and GHSR1a-negative (GHSR1a-) neurons. Ca_V currents were inhibited by 100 μM $CdCl_2$ (% of inhibition: GHSR1a+ = 99.91 ± 2.51 %, n = 5; GHSR1a- = 99.28 ± 0.98 %, n = 5, both n.s. vs. 100%; t-test, $p > 0.05$). Ca_V currents recorded in GHSR1a+ neurons displayed the same voltage-dependency as those recorded in GHSR1a- neurons but they were significantly smaller (Figure 5A and B). Importantly, ghrelin application inhibited Ca_V currents in GHSR1a+ but not in GHSR1a- neurons (Figure 5A) and the effect was insensitive to + 80 mV pre-pulse application in agreement with our data in the expression system (% of I_{Ba} inhibition by ghrelin without +80 mV pre-pulse= 28.14 ± 6.16 and with +80 mV pre-pulse= 26.22 ± 7.27, n.s. n= 4 neurons, p= 0.57, paired t-test). We used ω-conotoxin-GVIA and ω-agatoxin-IVA to quantify the contribution of N- ($Ca_V2.2$) and P/Q-type ($Ca_V2.1$) channels, respectively, in this experimental system. We found that both current subtypes were significantly smaller in GHSR1a+ compared to GHSR1a- neurons in the presence or absence of ghrelin (Figure 5C). However, TTX-sensitive Na_V currents in GHSR1a+ and GHSR1a- neurons were not different (t-test, $p > 0.05$, Figure 5D). Thus,

GHSR1a+ neurons have reduced N- and P/Q-type currents as compared to GHSR1a- neurons, and ghrelin inhibits those currents only in GHSR1a+ neurons.

In order to dissociate the effect of constitutive and ghrelin-dependent GHSR1a activities on native calcium channels, we transfected either GHSR1a-YFP or GHSR1a-A204E-YFP in hypothalamic rat cultured neurons, which express minimal levels of endogenous GHSR1a under our experimental conditions (6 ± 2 % of neurons bind F-ghrelin, n = 3 independent cultures). Ca_V currents recorded in neurons expressing GHSR1a-YFP were significantly smaller as compared to those recorded in either neurons expressing eGFP or GHSR1a-A204E-YFP neurons (Figure 6A). Ghrelin inhibited the same relative percentage of Ca_V currents in neurons expressing either GHSR1a-YFP or GHSR1a-A204E-YFP while it failed to affect Ca_V currents in neurons expressing eGFP or non-transfected neurons (Figure 6B, normalized current traces). We next used ω-conotoxin-GVIA and ω-agatoxin-IVA to test Ca_V2 subtypes contribution to the total Ca_V current in our experimental conditions. We found a smaller contribution of $Ca_V2.1$ and $Ca_V2.2$ in GHSR1a-YFP expressing neurons as compared to the contribution found in GHSR1a-A204E-YFP expressing neurons. Additionally, calcium currents in presence of ghrelin showed a reduced contribution of Ca_V2 in both GHSR1a-YFP and GHSR1a-A204E-YFP expressing neurons (Figure 6C). Importantly, TTX-sensitive Na_V currents were not affected among the different experimental conditions (Figure 6D). Thus, constitutive and ghrelin-dependent GHSR1a activities inhibit native N- and P/Q-type calcium currents in hypothalamic neurons.

Constitutive and ghrelin-dependent GHSR1a activities reduce GABA release from hypothalamic explants

In previous studies we have suggested that GHSR1a activity decreases inhibitory tone on hypothalamic neurons (Cabral et al., 2012). Thus, we next evaluated if GHSR1a

activity affects GABA release from explants of the arcuate nucleus (ARC), an hypothalamic nucleus where GHSR1a is highly expressed (Zigman et al., 2006) and GABA release is essential for food intake regulation (Wu et al., 2009). In order to explore the role of constitutive GHSR1a activity, we used 48 h fasted mice, in which hypothalamic GHSR1a mRNA levels were 1.5-fold higher in comparison to levels found in *ad libitum* fed mice (Figure 7A, right). We studied the [3H]-GABA release from explants of ARC and we found a significant reduction of [3H]-GABA release stimulated by high K^+ in explants from fasted mice as compared to release detected in explants from *ad libitum* fed mice (Figure 7A, left). Thus, our data show that fasting-induced increase of GHSR1a expression levels correlates with an inhibition of GABA release from ARC neurons.

In order to test if constitutive GHSR1a activity-displayed inhibition of N- and P/Q-type currents impacts on GABA release, we recorded IPSCs in hypothalamic neuronal cultures from GHSR null mice transduced with either GHSR1a-YFP or GHSR1a-A204E-YFP lentiviral vectors, which allow a high percentage of GHSR1a expressing neurons. In these experimental conditions, we found a reduced IPSC size triggered by electrical stimulation in GHSR1a-YFP expressing cultures in comparison with both GHSR1a-A204E-YFP expressing cultures and non-transduced cultures (Figure 7B). Moreover, we found that acute ghrelin application reduced ~ 20 % the IPSC peak in cultures expressing either GHSR1a-YFP or GHSR1a-A204E-YFP (Figure 7C, normalized IPSC recordings), indicating that both GHSR1a variants are functional and that ghrelin-dependent GHSR1a activation can further inhibit IPSCs. Finally, we recorded GABAergic postsynaptic responses stimulated by hyperosmotic solution in presence of TTX, a maneuver known to release neurotransmitter in a Ca_V-independent manner. We found no differences in these responses among non-transduced, GHSR1a-YFP transduced and GHSR1a-A204E-YFP transduced cultures suggesting that constitutive GHSR1a activity exclusively affects action potential dependent and Ca_V2-mediated GABAergic neurotransmission. Importantly, the

size of spontaneous IPSCs was not different among conditions (Figure 7D) indicating the lack of a postsynaptic effects in the IPSC size reduction by GHSR1a activity.

Discussion

We present evidence that GHSR1a, the GPCR with the highest constitutive activity, down-regulates $Ca_V2.1$ and $Ca_V2.2$ currents by a mechanism that is independent of its endogenous agonist, ghrelin, and involves $G_{i/o}$ signaling and plasma membrane channel density reduction. We also show that ghrelin inhibits native and cloned $Ca_V2.1$ and $Ca_V2.2$ currents via activation of GHSR1a by a different signaling cascade that involves G_q protein activation. These two fundamentally different mechanisms could differentially contribute to regulate presynaptic Ca^{2+} entry and transmitter release from hypothalamic neurons.

Presynaptic Ca_V2 channels inhibition by GPCRs is an important mechanism mediating the effects of many transmitters and drugs that control neurotransmitter release (Catterall and Few, 2008). GHSR1a is expressed at axonal terminals and a presynaptic role for this receptor has been suggested (Cowley et al., 2003; Cui et al., 2011; Yang et al., 2011; Ribeiro et al., 2014). In general, ghrelin/GHSR1a system stimulates electrical and transcriptional activity in neurons (Cowley et al., 2003; Andrews et al., 2009; Shi et al., 2013). Also, it has been shown that GHSR1a signaling augments cytosolic Ca^{2+} levels in hypothalamic neurons (Howard et al., 1996; Chuang et al., 2011b; Yang et al., 2011). Here, we propose a novel mechanism that could potentially contribute to neuronal activation of hypothalamic neurons by controlling Ca_V2 channels located at the presynaptic terminals of inhibitory input neurons. Moreover, in agreement with previous data showing that GHSR1a can couple to several different pathways, we demonstrate that two fundamentally different mechanisms govern ghrelin-dependent and ghrelin-independent Ca_V2 inhibition by GHSR1a.

We show evidence that constitutive GHSR1a activity down regulates Ca_V2 channel density by a $G_{i/o}$-dependent signaling pathway. GHSR1a is typically thought to involve G_q protein activation (Holst et al., 2003) although $G_{i/o}$ involvement is also well documented

(Bennett et al., 2009). Other GPCRs, such as the nociceptin receptor (opioid receptor-like receptor, ORL1) and metabotropic glutamate receptor subtype 1 (mGluR1), have been shown to inhibit Ca_V2 by agonist binding independent mechanisms that require GPCR and channel protein direct interaction (Kitano et al., 2003; Beedle et al., 2004). ORL1 is a $G_{i/o}$ coupled receptor that inhibits $Ca_V2.2$ channels in dorsal root ganglion neurons, and it has been shown that basal and nociceptin-mediated ORL1 inhibition of $Ca_V2.2$ shared a $G_{\beta\gamma}$-mediated pathway since both are avoided by $G_{\beta\gamma}$ sequestering or depolarizing pre-pulse voltage application (Beedle et al., 2004). In contrast, here we show that Ca_V2 current inhibition by constitutive GHSR1a activity differs from ghrelin-evoked effect as the former mode of inhibition is independent of $G_{\beta\gamma}$ binding and unaffected by a depolarizing pre-pulse.

The long-lasting inhibition of Ca_V2 currents by GHSR1a constitutive activity implicates channel density reduction at the plasma membrane. Several GPCRs, including dopamine receptors and ORL1 utilize mechanisms involving channel internalization to impact on Ca_V2 currents in the long term (Altier et al., 2006; Kisilevsky et al., 2008; Kisilevsky and Zamponi, 2008). In a clear demonstration of complexity in channel activity regulation by GPCRs these receptors can inhibit the channels by voltage-dependent and voltage-independent modulation and also, by co-internalization resulting from direct interaction between the activated receptor and the channel. We cannot discard the direct interaction between the GHSR1a and Ca_V2 channels in the mechanism involved in channel density reduction by GHSR1a constitutive activity. If present, however, this mechanism is likely insufficient to mediate channel density reduction since protein $G_{i/o}$ activation is required for the effect. The molecular mechanism by which GHSR1a-mediated $G_{i/o}$ basal activation modifies channel density is unclear with our present data. We postulate that a reduced channel trafficking as a more suitable hypothesis over channel internalization, given the long-term effect of the GHSR1a inverse agonist (see

Figure 2B) and the particular distribution of fluorescence signal from Ca_V2-GFP around the nucleus of transfected HEK 293T cells (see Figure 4A). More experiments are required in order to determine the intermediate molecular players of this pathway. Thus, there is increasing evidence that channel trafficking regulation from and toward the plasma membrane could be universal mechanisms that GPCRs utilize to control voltage-gated calcium currents in neurons.

We found that ghrelin-dependent GHSR1a activity inhibits Ca_V2 channel by a rapid and reversible G_q-dependent signaling pathway. G_q activation generally inhibits Ca_V2 in a voltage-independent manner. Several signaling pathways have been proposed to mediate calcium channel inhibition including PtdIns(4,5)P_2 (PIP_2) depletion from plasma membrane, increase of arachidonic acid production and protein kinases activation (Wu et al., 2002; Liu and Rittenhouse, 2003; Gamper et al., 2004; Suh et al., 2010). The Ca_V2 inhibition induced by PIP_2 depletion or arachidonic acid increment requires cytoplasmic subtypes of $Ca_V\beta$ ($Ca_V\beta_3$) and, as a consequence, both mechanisms fail to impair Ca_V2 currents if channels contain the membrane anchored form of $Ca_V\beta$, $Ca_V\beta_{2a}$ (Heneghan et al., 2009; Suh et al., 2012). Accordingly, we found that the inhibition of $Ca_V2.2$ induced by ghrelin-evoked GHSR1a activation depends on the type of $Ca_V\beta$ subunit. In particular, the ghrelin-mediated $Ca_V2.2$ inhibition was significantly reduced and fully voltage-dependent when $Ca_V\beta_{2a}$ was present while it was larger and voltage-independent in the presence of $Ca_V\beta_3$. Additionally, we found that buffering $G_{\beta\gamma}$ is enough to completely avoid the ghrelin-mediated inhibition of $Ca_V2.2$ independently of the $Ca_V\beta$ subtype. Previous reports have shown the same dependency of $G_{\beta\gamma}$ for other G_qPCRs-mediated pathways (i.e. muscarinic type 1 and neurokinin type 1 receptors) (Kammermeier et al., 2000). Thus, our data support the notion that $Ca_V\beta_{2a}$ in the channel complex switches the voltage dependency of

Ca_V2 inhibition by occluding G_q subunit signaled effect and unmasks the inhibition by $G_{\beta\gamma}$ direct binding as recently demonstrated by Keum and colleagues (Keum et al., 2014).

Peripheral administration of ghrelin potently increases food intake (Nakazato et al., 2001). Plasma ghrelin almost exclusively access the hypothalamic ARC, which expresses high levels of GHSR1a and is required for the orexigenic actions of peripheral ghrelin (Zigman et al., 2006; Schaeffer et al., 2013; Cabral et al., 2014). GABA release from ARC neurons is essential for food intake regulation (Wu et al., 2009) and GHSR1a is found at presynaptic terminals (Cowley et al., 2003; Yang et al., 2011). It has been also shown that GABA release by AgRP ARC neurons is required for ghrelin-induced food intake (Tong et al., 2008), and a ghrelin-induced reduction of GABA release has been proposed to mediate other hypothalamic actions of the hormone (Cabral et al., 2012). Thus, current results showing that ghrelin-induced GHSR1a activity inhibits native calcium channels, impairs Ca_V2 dependent GABA release from ARC explants and modify synaptic activity in hypothalamic neurons in culture offer a molecular mechanism that could mediate well established effects of ghrelin. In contrast, the physiological role of constitutive GHSR1a activity has been hard to highlight in *in vivo* settings. Here, we confirmed that GHSR1a expression level is affected by the energy balance conditions, and found that this change correlates with GABA release from ARC explants suggesting that GHSR1a constitutive activity may have functional implications (Holst et al., 2003; Kim et al., 2003; Pantel et al., 2006; Kineman and Luque, 2007; Liu et al., 2007). The facts that *in vivo* administration of the GHSR1a inverse agonist SPA reduces food intake and body weight in rats (Petersen et al., 2009), and that mice lacking GHSR1a exhibit a more severe phenotype as compared to ghrelin knockout mice have been also interpreted as indications of a physiological role of the constitutive GHSR1a activity (Uchida et al., 2013). Notably, the A204E mutation has been associated with short stature and dominant transmission in

human beings (Pantel et al., 2006). However, further studies are required in order to explore the physiological implications of the GHSR1a-related molecular events that occur in a ghrelin-independent fashion.

Current data open many intriguing questions including the physiological relevance of constitutive activity at synapses without ghrelin availability and mechanisms that regulate the agonist independent actions of GHSR1a. Interestingly, GHSR1a is also present in brain areas distant from circumventricular organs (Zigman et al., 2006) that are not accessed by plasma ghrelin (Cabral et al., 2013; Cabral et al., 2014). It has been proposed that GHSR1a located in obvious inaccessible areas to plasma ghrelin could be modulated by centrally-produced ghrelin (Cowley et al., 2003); however, more recent studies have clearly shown that ghrelin is not synthesized in the central nervous system (Sakata et al., 2009; Furness et al., 2011). Besides receptor expression levels, hetero-dimerization of GHSR1a with other GPCRs could also serve as an alternative mechanism to modulate specific functions of this receptor, independently of ghrelin binding (Jiang et al., 2006; Rediger et al., 2011; Kern et al., 2012; Schellekens et al., 2013). Thus, more efforts will be required to get insight on the complexity of the GHSR1a/ghrelin actions in neurons.

Acknowledgements

This work was supported by grants from the National Agency of Scientific and Technological Promotion of Argentina (PICT2010-1954 and PICT2011-2142 to MP and PICT2011-1816 and PICT2013-1145 to JR) and NIH (R03TW008925-01A1 to MP). We thank Dr. Jeffrey Zigman for providing GHSR-GFP mice. EJLP, FA, AC, ERM and VMD were supported by CONICET and CIC-PBA's fellowships.

The authors declare no competing financial interests.

References

Agosti, F., E.J. Lopez Soto, A. Cabral, D. Castrogiovanni, H.B. Schioth, M. Perello, and J. Raingo. 2014. Melanocortin 4 receptor activation inhibits presynaptic N-type calcium channels in amygdaloid complex neurons. *Eur J Neurosci*. 40:2755-2765.

Altier, C., H. Khosravani, R.M. Evans, S. Hameed, J.B. Peloquin, B.A. Vartian, L. Chen, A.M. Beedle, S.S. Ferguson, A. Mezghrani, S.J. Dubel, E. Bourinet, J.E. McRory, and G.W. Zamponi. 2006. ORL1 receptor-mediated internalization of N-type calcium channels. *Nat Neurosci*. 9:31-40.

Andrews, Z.B., D. Erion, R. Beiler, Z.W. Liu, A. Abizaid, J. Zigman, J.D. Elsworth, J.M. Savitt, R. DiMarchi, M. Tschoep, R.H. Roth, X.B. Gao, and T.L. Horvath. 2009. Ghrelin promotes and protects nigrostriatal dopamine function via a UCP2-dependent mitochondrial mechanism. *J Neurosci*. 29:14057-14065.

Andrews, Z.B., Z.W. Liu, N. Walllingford, D.M. Erion, E. Borok, J.M. Friedman, M.H. Tschop, M. Shanabrough, G. Cline, G.I. Shulman, A. Coppola, X.B. Gao, T.L. Horvath, and S. Diano. 2008. UCP2 mediates ghrelin's action on NPY/AgRP neurons by lowering free radicals. *Nature*. 454:846-851.

Beedle, A.M., J.E. McRory, O. Poirot, C.J. Doering, C. Altier, C. Barrere, J. Hamid, J. Nargeot, E. Bourinet, and G.W. Zamponi. 2004. Agonist-independent modulation of N-type calcium channels by ORL1 receptors. *Nat Neurosci*. 7:118-125.

Bennett, K.A., C.J. Langmead, A. Wise, and G. Milligan. 2009. Growth hormone secretagogues and growth hormone releasing peptides act as orthosteric super-agonists but not allosteric regulators for activation of the G protein Galpha(o1) by the Ghrelin receptor. *Mol Pharmacol*. 76:802-811.

Cabral, A., G. Fernandez, and M. Perello. 2013. Analysis of brain nuclei accessible to ghrelin present in the cerebrospinal fluid. *Neuroscience*. 253:406-415.

Cabral, A., O. Suescun, J.M. Zigman, and M. Perello. 2012. Ghrelin indirectly activates hypophysiotropic CRF neurons in rodents. *PLoS One*. 7:e31462.

Cabral, A., S. Valdivia, G. Fernandez, M. Reynaldo, and M. Perello. 2014. Divergent neuronal circuitries underlying acute orexigenic effects of peripheral or central ghrelin: critical role of brain accessibility. *J Neuroendocrinol*.

Cao, Y.Q., E.S. Piedras-Renteria, G.B. Smith, G. Chen, N.C. Harata, and R.W. Tsien. 2004. Presynaptic Ca2+ channels compete for channel type-preferring slots in altered neurotransmission arising from Ca2+ channelopathy. *Neuron*. 43:387-400.

Catterall, W.A., and A.P. Few. 2008. Calcium channel regulation and presynaptic plasticity. *Neuron*. 59:882-901.

Cogger, V.C., G.P. McNerney, T. Nyunt, L.D. DeLeve, P. McCourt, B. Smedsrod, D.G. Le Couteur, and T.R. Huser. 2010. Three-dimensional structured illumination microscopy of liver sinusoidal endothelial cell fenestrations. *J Struct Biol*. 171:382-388.

Cowley, M.A., R.G. Smith, S. Diano, M. Tschop, N. Pronchuk, K.L. Grove, C.J. Strasburger, M. Bidlingmaier, M. Esterman, M.L. Heiman, L.M. Garcia-Segura, E.A. Nillni, P. Mendez, M.J. Low, P. Sotonyi, J.M. Friedman, H. Liu, S. Pinto, W.F. Colmers, R.D. Cone, and T.L. Horvath. 2003. The distribution and mechanism of action of ghrelin in the CNS demonstrates a novel hypothalamic circuit regulating energy homeostasis. *Neuron*. 37:649-661.

Cui, R.J., X. Li, and S.M. Appleyard. 2011. Ghrelin inhibits visceral afferent activation of catecholamine neurons in the solitary tract nucleus. *J Neurosci*. 31:3484-3492.

Chuang, J.C., M. Perello, I. Sakata, S. Osborne-Lawrence, J.M. Savitt, M. Lutter, and J.M. Zigman. 2011a. Ghrelin mediates stress-induced food-reward behavior in mice. *J Clin Invest*. 121:2684-2692.

Chuang, J.C., I. Sakata, D. Kohno, M. Perello, S. Osborne-Lawrence, J.J. Repa, and J.M. Zigman. 2011b. Ghrelin directly stimulates glucagon secretion from pancreatic alpha-cells. *Mol Endocrinol*. 25:1600-1611.

Diano, S., S.A. Farr, S.C. Benoit, E.C. McNay, I. da Silva, B. Horvath, F.S. Gaskin, N. Nonaka, L.B. Jaeger, W.A. Banks, J.E. Morley, S. Pinto, R.S. Sherwin, L. Xu, K.A. Yamada, M.W. Sleeman, M.H. Tschop, and T.L. Horvath. 2006. Ghrelin controls hippocampal spine synapse density and memory performance. *Nat Neurosci*. 9:381-388.

Evron, T., S.M. Peterson, N.M. Urs, Y. Bai, L.K. Rochelle, M.G. Caron, and L.S. Barak. 2014. G Protein and beta-Arrestin Signaling Bias at the Ghrelin Receptor. *J Biol Chem*. 289:33442-33455.

Furness, J.B., B. Hunne, N. Matsuda, L. Yin, D. Russo, I. Kato, M. Fujimiya, M. Patterson, J. McLeod, Z.B. Andrews, and R. Bron. 2011. Investigation of the presence of ghrelin in the central nervous system of the rat and mouse. *Neuroscience*. 193:1-9.

Gamper, N., V. Reznikov, Y. Yamada, J. Yang, and M.S. Shapiro. 2004. Phosphatidylinositol [correction] 4,5-bisphosphate signals underlie receptor-specific Gq/11-mediated modulation of N-type Ca2+ channels. *J Neurosci*. 24:10980-10992.

Gandini, M.A., D.R. Henriquez, L. Grimaldo, A. Sandoval, C. Altier, G.W. Zamponi, R. Felix, and C. Gonzalez-Billault. 2014. CaV2.2 channel cell surface expression is regulated by the light chain 1 (LC1) of the microtubule-associated protein B (MAP1B) via UBE2L3-mediated ubiquitination and degradation. *Pflugers Arch*. 466:2113-2126.

Heneghan, J.F., T. Mitra-Ganguli, L.F. Stanish, L. Liu, R. Zhao, and A.R. Rittenhouse. 2009. The Ca2+ channel beta subunit determines whether stimulation of Gq-coupled receptors enhances or inhibits N current. *J Gen Physiol*. 134:369-384.

Holst, B., A. Cygankiewicz, T.H. Jensen, M. Ankersen, and T.W. Schwartz. 2003. High constitutive signaling of the ghrelin receptor--identification of a potent inverse agonist. *Mol Endocrinol*. 17:2201-2210.

Howard, A.D., S.D. Feighner, D.F. Cully, J.P. Arena, P.A. Liberator, C.I. Rosenblum, M. Hamelin, D.L. Hreniuk, O.C. Palyha, J. Anderson, P.S. Paress, C. Diaz, M. Chou, K.K. Liu, K.K. McKee, S.S. Pong, L.Y. Chaung, A. Elbrecht, M. Dashkevicz, R. Heavens, M. Rigby, D.J. Sirinathsinghji, D.C. Dean, D.G. Melillo, A.A. Patchett, R. Nargund, P.R. Griffin, J.A. DeMartino, S.K. Gupta, J.M. Schaeffer, R.G. Smith, and L.H. Van der Ploeg. 1996. A receptor in pituitary and hypothalamus that functions in growth hormone release. *Science*. 273:974-977.

Ikeda, S.R. 1996. Voltage-dependent modulation of N-type calcium channels by G-protein beta gamma subunits. *Nature*. 380:255-258.

Jiang, H., L. Betancourt, and R.G. Smith. 2006. Ghrelin amplifies dopamine signaling by cross talk involving formation of growth hormone secretagogue receptor/dopamine receptor subtype 1 heterodimers. *Mol Endocrinol*. 20:1772-1785.

Jiang, M., and G. Chen. 2006. High Ca2+-phosphate transfection efficiency in low-density neuronal cultures. *Nat Protoc*. 1:695-700.

Kammermeier, P.J., and S.R. Ikeda. 1999. Expression of RGS2 alters the coupling of metabotropic glutamate receptor 1a to M-type K+ and N-type Ca2+ channels. *Neuron*. 22:819-829.

Kammermeier, P.J., V. Ruiz-Velasco, and S.R. Ikeda. 2000. A voltage-independent calcium current inhibitory pathway activated by muscarinic agonists in rat sympathetic neurons requires both Galpha q/11 and Gbeta gamma. *J Neurosci*. 20:5623-5629.

Kern, A., R. Albarran-Zeckler, H.E. Walsh, and R.G. Smith. 2012. Apo-ghrelin receptor forms heteromers with DRD2 in hypothalamic neurons and is essential for anorexigenic effects of DRD2 agonism. *Neuron*. 73:317-332.

Keum, D., C. Baek, D.I. Kim, H.J. Kweon, and B.C. Suh. 2014. Voltage-dependent regulation of CaV2.2 channels by Gq-coupled receptor is facilitated by membrane-localized beta subunit. *J Gen Physiol*. 144:297-309.

Kim, M.S., C.Y. Yoon, K.H. Park, C.S. Shin, K.S. Park, S.Y. Kim, B.Y. Cho, and H.K. Lee. 2003. Changes in ghrelin and ghrelin receptor expression according to feeding status. *Neuroreport*. 14:1317-1320.

Kineman, R.D., and R.M. Luque. 2007. Evidence that ghrelin is as potent as growth hormone (GH)-releasing hormone (GHRH) in releasing GH from primary pituitary cell cultures of a nonhuman primate (Papio anubis), acting through intracellular signaling pathways distinct from GHRH. *Endocrinology*. 148:4440-4449.

Kisilevsky, A.E., S.J. Mulligan, C. Altier, M.C. Iftinca, D. Varela, C. Tai, L. Chen, S. Hameed, J. Hamid, B.A. Macvicar, and G.W. Zamponi. 2008. D1 receptors physically interact with N-type calcium channels to regulate channel distribution and dendritic calcium entry. *Neuron*. 58:557-570.

Kisilevsky, A.E., and G.W. Zamponi. 2008. D2 dopamine receptors interact directly with N-type calcium channels and regulate channel surface expression levels. *Channels (Austin)*. 2:269-277.

Kitano, J., M. Nishida, Y. Itsukaichi, I. Minami, M. Ogawa, T. Hirano, Y. Mori, and S. Nakanishi. 2003. Direct interaction and functional coupling between metabotropic glutamate receptor subtype 1 and voltage-sensitive Cav2.1 Ca2+ channel. *J Biol Chem*. 278:25101-25108.

Kurrasch, D.M., J. Huang, T.M. Wilkie, and J.J. Repa. 2004. Quantitative real-time polymerase chain reaction measurement of regulators of G-protein signaling mRNA levels in mouse tissues. *Methods Enzymol*. 389:3-15.

Lauckner, J.E., B. Hille, and K. Mackie. 2005. The cannabinoid agonist WIN55,212-2 increases intracellular calcium via CB1 receptor coupling to Gq/11 G proteins. *Proc Natl Acad Sci U S A*. 102:19144-19149.

Lipscombe, D., S.E. Allen, and C.P. Toro. 2013. Control of neuronal voltage-gated calcium ion channels from RNA to protein. *Trends Neurosci*. 36:598-609.

Liu, G., J.P. Fortin, M. Beinborn, and A.S. Kopin. 2007. Four missense mutations in the ghrelin receptor result in distinct pharmacological abnormalities. *J Pharmacol Exp Ther*. 322:1036-1043.

Liu, L., and A.R. Rittenhouse. 2003. Arachidonic acid mediates muscarinic inhibition and enhancement of N-type Ca2+ current in sympathetic neurons. *Proc Natl Acad Sci U S A*. 100:295-300.

Lopez Soto, E.J., and J. Raingo. 2012. A118G Mu Opioid Receptor polymorphism increases inhibitory effects on CaV2.2 channels. *Neurosci Lett*. 523:190-194.

Mani, B.K., A.K. Walker, E.J. LopezSoto, J. Raingo, C.E. Lee, M. Perello, Z.B. Andrews, and J.M. Zigman. 2014. Neuroanatomical characterization of a growth hormone secretagogue receptor-green fluorescent protein reporter mouse. *J Comp Neurol*.

McGirr, R., M.S. McFarland, J. McTavish, L.G. Luyt, and S. Dhanvantari. 2011. Design and characterization of a fluorescent ghrelin analog for imaging the growth hormone secretagogue receptor 1a. *Regul Pept*. 172:69-76.

Nakazato, M., N. Murakami, Y. Date, M. Kojima, H. Matsuo, K. Kangawa, and S. Matsukura. 2001. A role for ghrelin in the central regulation of feeding. *Nature*. 409:194-198.

Pantel, J., M. Legendre, S. Cabrol, L. Hilal, Y. Hajaji, S. Morisset, S. Nivot, M.P. Vie-Luton, D. Grouselle, M. de Kerdanet, A. Kadiri, J. Epelbaum, Y. Le Bouc, and S. Amselem. 2006. Loss of constitutive activity of the growth hormone secretagogue receptor in familial short stature. *J Clin Invest*. 116:760-768.

Paxinos, G., and K. Franklin. 2001. The mouse brain-Second Edition. *Academic Press*.

Petersen, P.S., D.P. Woldbye, A.N. Madsen, K.L. Egerod, C. Jin, M. Lang, M. Rasmussen, A.G. Beck-Sickinger, and B. Holst. 2009. In vivo characterization of high Basal signaling from the ghrelin receptor. *Endocrinology*. 150:4920-4930.

Raingo, J., A.J. Castiglioni, and D. Lipscombe. 2007. Alternative splicing controls G protein-dependent inhibition of N-type calcium channels in nociceptors. *Nat Neurosci*. 10:285-292.

Raingo, J., M. Khvotchev, P. Liu, F. Darios, Y.C. Li, D.M. Ramirez, M. Adachi, P. Lemieux, K. Toth, B. Davletov, and E.T. Kavalali. 2012. VAMP4 directs synaptic vesicles to a pool that selectively maintains asynchronous neurotransmission. *Nat Neurosci*. 15:738-745.

Rediger, A., C.L. Piechowski, C.X. Yi, P. Tarnow, R. Strotmann, A. Gruters, H. Krude, T. Schoneberg, M.H. Tschop, G. Kleinau, and H. Biebermann. 2011. Mutually opposite signal modulation by hypothalamic heterodimerization of ghrelin and melanocortin-3 receptors. *J Biol Chem*. 286:39623-39631.

Ribeiro, L.F., T. Catarino, S.D. Santos, M. Benoist, J.F. van Leeuwen, J.A. Esteban, and A.L. Carvalho. 2014. Ghrelin triggers the synaptic incorporation of AMPA receptors in the hippocampus. *Proc Natl Acad Sci U S A*. 111:E149-158.

Sakata, I., Y. Nakano, S. Osborne-Lawrence, S.A. Rovinsky, C.E. Lee, M. Perello, J.G. Anderson, R. Coppari, G. Xiao, B.B. Lowell, J.K. Elmquist, and J.M. Zigman. 2009. Characterization of a novel ghrelin cell reporter mouse. *Regul Pept*. 155:91-98.

Schaeffer, M., F. Langlet, C. Lafont, F. Molino, D.J. Hodson, T. Roux, L. Lamarque, P. Verdie, E. Bourrier, B. Dehouck, J.L. Baneres, J. Martinez, P.F. Mery, J. Marie, E. Trinquet, J.A. Fehrentz, V. Prevot, and P. Mollard. 2013. Rapid sensing of circulating ghrelin by hypothalamic appetite-modifying neurons. *Proc Natl Acad Sci U S A*. 110:1512-1517.

Schellekens, H., W.E. van Oeffelen, T.G. Dinan, and J.F. Cryan. 2013. Promiscuous dimerization of the growth hormone secretagogue receptor (GHS-R1a) attenuates ghrelin-mediated signaling. *J Biol Chem*. 288:181-191.

Shi, L., X. Bian, Z. Qu, Z. Ma, Y. Zhou, K. Wang, H. Jiang, and J. Xie. 2013. Peptide hormone ghrelin enhances neuronal excitability by inhibition of Kv7/KCNQ channels. *Nat Commun*. 4:1435.

Suh, B.C., D.I. Kim, B.H. Falkenburger, and B. Hille. 2012. Membrane-localized beta-subunits alter the PIP2 regulation of high-voltage activated Ca2+ channels. *Proc Natl Acad Sci U S A*. 109:3161-3166.

Suh, B.C., K. Leal, and B. Hille. 2010. Modulation of high-voltage activated Ca(2+) channels by membrane phosphatidylinositol 4,5-bisphosphate. *Neuron*. 67:224-238.

Tong, Q., C.P. Ye, J.E. Jones, J.K. Elmquist, and B.B. Lowell. 2008. Synaptic release of GABA by AgRP neurons is required for normal regulation of energy balance. *Nat Neurosci*. 11:998-1000.

Uchida, A., J.M. Zigman, and M. Perello. 2013. Ghrelin and eating behavior: evidence and insights from genetically-modified mouse models. *Front Neurosci*. 7:121.

Wu, L., C.S. Bauer, X.G. Zhen, C. Xie, and J. Yang. 2002. Dual regulation of voltage-gated calcium channels by PtdIns(4,5)P2. *Nature*. 419:947-952.

Wu, Q., M.P. Boyle, and R.D. Palmiter. 2009. Loss of GABAergic signaling by AgRP neurons to the parabrachial nucleus leads to starvation. *Cell*. 137:1225-1234.

Yang, Y., D. Atasoy, H.H. Su, and S.M. Sternson. 2011. Hunger states switch a flip-flop memory circuit via a synaptic AMPK-dependent positive feedback loop. *Cell*. 146:992-1003.

Yu, B., and M.I. Simon. 1998. Interaction of the xanthine nucleotide binding Goalpha mutant with G protein-coupled receptors. *J Biol Chem*. 273:30183-30188.
Zamponi, G.W., and K.P. Currie. 2013. Regulation of Ca(V)2 calcium channels by G protein coupled receptors. *Biochim Biophys Acta*. 1828:1629-1643.
Zigman, J.M., J.E. Jones, C.E. Lee, C.B. Saper, and J.K. Elmquist. 2006. Expression of ghrelin receptor mRNA in the rat and the mouse brain. *J Comp Neurol*. 494:528-548.

FIGURE LEGENDS

Figure 1. Constitutive and ghrelin-dependent GHSR1a activity inhibit Ca_V2 currents. **A-** Representative I_{Ca} traces from HEK 293T cells transfected with $Ca_V2.1$ or $Ca_V2.2$, $Ca_V\alpha_2\delta_1$, $Ca_V\beta_3$ and 0.6 µg of GHSR1a, GHSR1a-A204E or empty pcDNA3.1+ (control), and averaged I_{Ca} at different amounts of GHSR1a plasmid transfected. **B-** Representative microphotographies (left) and average fluorescent signal intensity (right) for the F-ghrelin binding in cells transfected with increasing amounts of GHSR1a plasmid. **C-** Representative I_{Ca} traces from cells co-transfected with $Ca_V2.1$ and $Ca_V2.2$, $Ca_V\alpha_2\delta_1$, $Ca_V\beta_3$ and 0.6 µg of GHSR1a or GHSR1a-A204E with or without 1 µM SPA pre-incubation (left), and the averaged I_{Ca} for each condition (right). **D-** Time courses and representative traces of ghrelin effect on I_{Ca} from cells expressing $Ca_V2.1$ or $Ca_V2.2$, $Ca_V\alpha_2\delta_1$, $Ca_V\beta_3$ and GHSR1a-A204E (left), and the averaged % $Ca_V2.1$ and $Ca_V2.2$ current inhibition at different amounts of GHSR1a plasmid transfected. ANOVA with Dunnett's (panel C) and Tukey's post-test (panel D). * $p < 0.05$.

Figure 2. Constitutive GHSR1a activity inhibits by a long term mechanism the Ca_V2 currents preserving Ca_V2 current inhibition by ghrelin-dependent GHSR1a activity. **A-** Representative I_{Ca} traces (left) from HEK 293T cells expressing $Ca_V2.1$ (above) or $Ca_V2.2$ (below), $Ca_V\alpha_2\delta_1$, $Ca_V\beta_3$ and GHSR1a pre-incubated with 1 µM SPA, before (control) and after (+ghrelin) 500 nM ghrelin application; and averaged % of I_{Ca} inhibition by 500 nM

ghrelin (right) from HEK 293T cells expressing $Ca_V2.1$ or $Ca_V2.2$, $Ca_V\alpha_2\delta_1$, $Ca_V\beta_3$ and GHSR1a pre-incubated with 1 μM SPA or GHSR1a-A204E as control condition. **B-** Time courses of peak Ca_V2 currents (left) with the acute application of 1 μM SPA (gray bars) from HEK 293T cells expressing $Ca_V2.1$ (above) or $Ca_V2.2$ (below), $Ca_V\alpha_2\delta_1$, $Ca_V\beta_3$ and GHSR1a, and the averaged $Ca_V2.1$ or $Ca_V2.2$ currents before (control) and after (+SPA) acute application of 1 μM SPA. Two sample (panel A) and paired (panel B) Student's t-test.

Figure 3. $Ca_V2.2$ inhibition by constitutive and ghrelin-dependent GHSR1a activity are signaled by $G_{i/o}$ and G_q proteins, respectively. **A-** Time course, representative traces and averaged I_{Ca} inhibition by 500 nM ghrelin in HEK 293T cells transfected with $Ca_V2.2$, $Ca_V\alpha_2\delta_1$, $Ca_V\beta_3$ and GHSR1a-A204E in control conditions or pre-incubated with 500 ng/ml of Cholera toxin (ChTx) or 500 ng/ml of Pertussis toxin (PTx), or co-transfected with a G_q dominant negative mutant (G_qDN). **B-** Representative traces and averaged I_{Ca} in HEK 293T cells expressing $Ca_V2.2$, $Ca_V\alpha_2\delta_1$, $Ca_V\beta_3$ and GHSR1a or GHSR1a-A204E, in control or pre-incubated with 500 ng/ml of ChTx or 500 ng/ml of PTx, or co-transfected with G_qDN. **C-** Representative traces and averaged I_{Ca} inhibition by 500 nM ghrelin in HEK 293T cells transfected with $Ca_V2.2$, $Ca_V\alpha_2\delta_1$, $Ca_V\beta_3$ and GHSR1a pre-incubated with 500 ng/ml of Pertussis toxin (PTx). **D-** Representative I_{Ca} in HEK 293T cells co-transfected with $Ca_V2.2$, $Ca_V\alpha_2\delta_1$, GHSR1a-A204E and $Ca_V\beta_3$ or $Ca_V\beta_{2a}$ without (control) or with (+ghrelin) 500 nM ghrelin without or with (+pp) a +80 mV pre-pulse application (left) and; averaged % of I_{Ca} inhibition by 500 nM ghrelin in cells expressing $Ca_V2.2$, $Ca_V\alpha_2\delta_1$ and GHSR1a-A204E with the co-expression of $Ca_V\beta_3$ or $Ca_V\beta_{2a}$ and MAS-GRK2-ct and pre-pulse application (+pp) (right). **E-** Representative I_{Ca} traces from cells co-transfected with $Ca_V2.2$, $Ca_V\alpha_2\delta_1$, $Ca_V\beta_3$ and GHSR1a or GHSR1a-A204E with (+pp) or without (Control) the application of +80 mV

pre-pulse (left) and averaged I_{Ca} from HEK 293T cells expressing $Ca_V2.2$, $Ca_V\alpha_2\delta_1$, GHSR1a or GHSR1a-A204E, with the co-expression of $Ca_V\beta_3$ or $Ca_V\beta_{2a}$ and MAS-GRK2ct and +80 mV pre-pulse application (+pp) (right). ANOVA with Dunnett's (panel A and B) or Tukey's post-test (panel D) and two sample Student's t-test (panel E). * $p < 0.05$.

Figure 4- GHSR1a decreases surface $Ca_V2.1$ and $Ca_V2.2$ density. **A-** Photomicrographs and averaged percentages of green fluorescent plasma membrane signal of HEK 293T cells transfected with $Ca_V2.1$-GFP (left) and $Ca_V2.2$-GFP (right), its auxiliary subunits (Control) with GHSR1a or GHSR1a-A204E, pre-incubated or not with 1 µM SPA or 500 ng/ml of PTx. Green and red signals correspond to the eGFP tag on Ca_V2 and the membrane marker CellMask™ respectively. Kruskal-Wallis with Dunns post-test, * $p < 0.01$. **B-** Western blot analysis displaying the $Ca_V2.1$-GFP and $Ca_V2.2$-GFP protein level in the plasma membrane (PM) or the cytoplasmic (Cyt) fraction of HEK 293T cells transfected with $Ca_V2.1$-GFP or $Ca_V2.2$-GFP and its auxiliary subunits (Control) and co-transfected with GHSR1a or GHSR1a-A204E (left) and averaged % of $Ca_V2.1$-GFP and $Ca_V2.2$-GFP PM protein level in each condition normalized against cadherin signal used as the plasma membrane loading control (right). Both AKT and Hsp90 as cytosolic markers. n = 2 and 3 for $Ca_V2.1$-GFP or $Ca_V2.2$-GFP, respectively.

Figure 5- GHSR1a activity modulates native Ca_V2 currents in hypothalamic neurons from GHSR-eGFP reporter mice. **A-** Representative I_{Ba} traces and averaged I_{Ba} before (control) and after (+ghrelin) 500 nM ghrelin application in hypothalamic GHSR1a- and GHSR1a+ neurons. **B-** Averaged peak I_{Ba} -voltage (IV) relationships (evoked from a holding of -80 mV), reversal (V_{rev}) and activation ($V_{1/2}$) potentials midpoints (calculated by Boltzmann-linear function) obtained from GHSR1a- and GHSR1a+ neurons. **C-** I_{Ba} time courses of

application of 1 μM ω-conotoxin-GVIA (conoTx) and 0.2 μM ω-agatoxin-IVA (agaTx) with or without previous 500 nM ghrelin application from hypothalamic GHSR1a- (top) and GHSR1a+ neurons (center and bottom) (left). Averaged % of I_{Ba} sensitive to agaTx and conoTx from GHSR1a- and GHSR1a+ neurons, with (+ghrelin) or without 500 nM ghrelin application (right). **D-** Representative and averaged I_{Na} from GHSR1a- and GHSR1a+ neurons. Paired (panel A) or two sample (panel B and D) Student's t-test and ANOVA with Dunnett's post-test (panel C). * $p < 0.05$.

Figure 6- GHSR1a activity inhibits native Ca_V2 currents from rat hypothalamic neurons. **A-** Representative and averaged I_{Ba} from non-transfected (nt) and GFP, GHSR1a-YFP and GHSR1a-A204E-YFP transfected neurons. **B-** Normalized I_{Ba} traces before (control) and after (+ghrelin) 500 nM ghrelin application and averaged % of I_{Ba} inhibition by ghrelin in each condition. **C-** I_{Ba} time courses of application of 1 μM ω-conotoxin-GVIA (conoTx) and 0.2 μM ω-agatoxin-IVA (agaTx) with or without previous 500 nM ghrelin application from GFP, GHSR1a and GHSR1a-A204E transfected neurons (left). Averaged % of I_{Ba} sensitive to agaTx and conoTx from non-transfected (nt), GFP, GHSR1a and GHSR1a-A204E transfected neurons, with (+ghrelin) or without 500 nM ghrelin application (right). **D-** Representative and averaged I_{Na} from non-transfected (nt) and GFP, GHSR1a and GHSR1a-A204E transfected neurons. ANOVA with Dunnett's post-test (panel A, B, C and D). * $p < 0.05$.

Figure 7- GHSR1a activity impacts on GABA release. **A-** [3H]-GABA release (left) and GHSR1a mRNA levels (right) from ARC-enriched explants from ad libitum fed or 48 h fasted mice. **B-** Representative traces and averaged IPSC size obtained from GHSR null primary cultured neurons transduced or not with GHSR1a-YFP and GHSR1a-A204E-YFP. **C-** Representative normalized traces with or without the application of 500 nM of ghrelin

and average values of percentage of IPSC inhibition by ghrelin obtained from GHSR null primary cultured neurons transduced or not with GHSR1a-YFP and GHSR1a-A204E-YFP. **D-** Distribution of mIPSC size and averaged values for mIPSC frequencies and charge movement by 0.5 M sucrose solution application in GHSR null primary cultured neurons transduced or not with GHSR1a-YFP and GHSR1a-A204E-YFP. Two sample Student's t-test (panel A) and ANOVA with Dunnett's post-test (B, C and D). * $p < 0.05$.

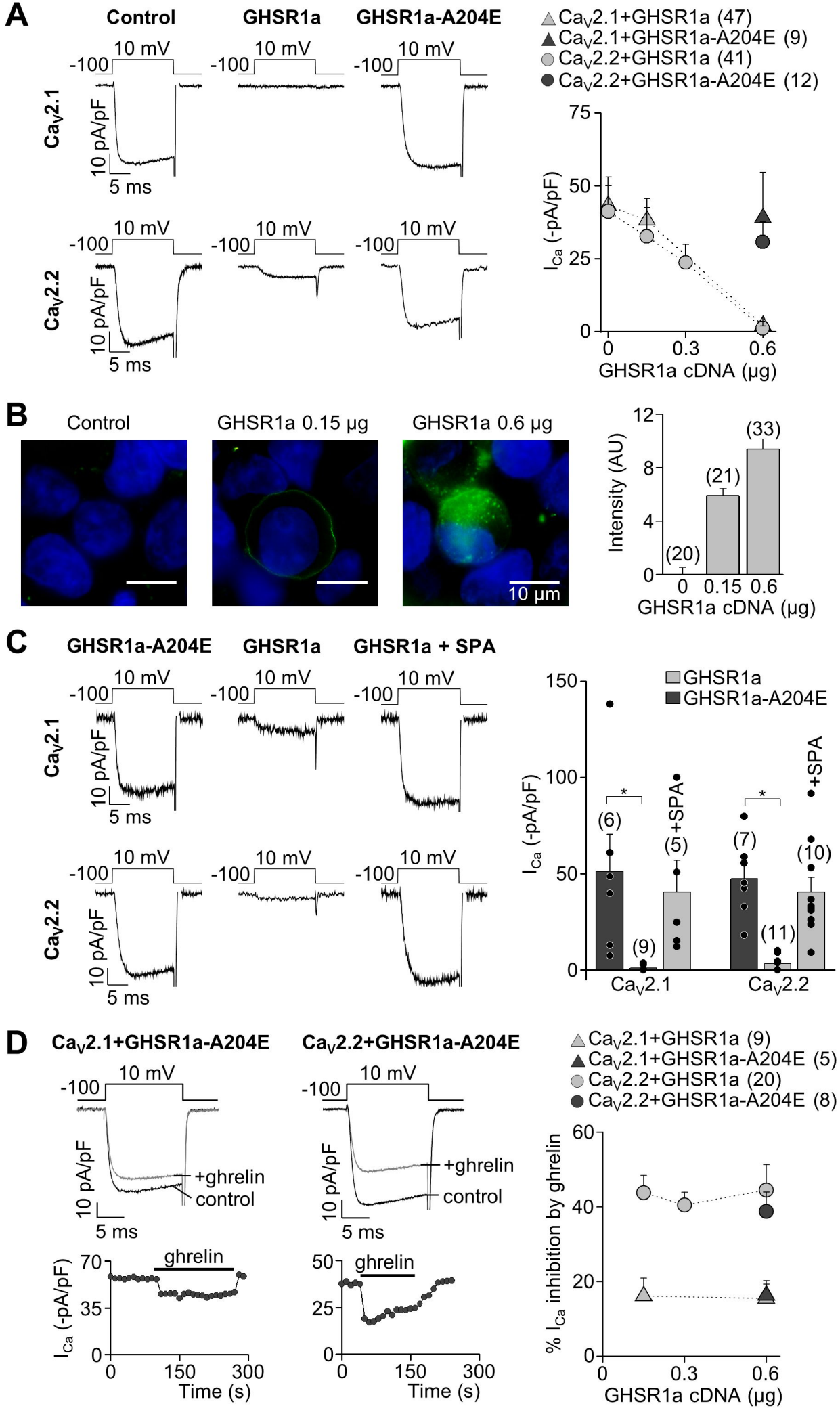
A
Control
GHSR1a
GHSR1a-A204E
10 mV
-100
10 pA/pF
5 ms
CaV2.1
CaV2.2
CaV2.1+GHSR1a (47)
CaV2.1+GHSR1a-A204E (9)
CaV2.2+GHSR1a (41)
CaV2.2+GHSR1a-A204E (12)
ICa (-pA/pF)
GHSR1a cDNA (µg)
B
Control
GHSR1a 0.15 µg
GHSR1a 0.6 µg
10 µm
Intensity (AU)
(20)
(21)
(33)
GHSR1a cDNA (µg)
C
GHSR1a-A204E
GHSR1a
GHSR1a + SPA
GHSR1a
GHSR1a-A204E
+SPA
(6)
(5)
(9)
(7)
(11)
(10)
CaV2.1
CaV2.2
D
CaV2.1+GHSR1a-A204E
CaV2.2+GHSR1a-A204E
+ghrelin
control
ghrelin
Time (s)
CaV2.1+GHSR1a (9)
CaV2.1+GHSR1a-A204E (5)
CaV2.2+GHSR1a (20)
CaV2.2+GHSR1a-A204E (8)
% ICa inhibition by ghrelin
GHSR1a cDNA (µg)

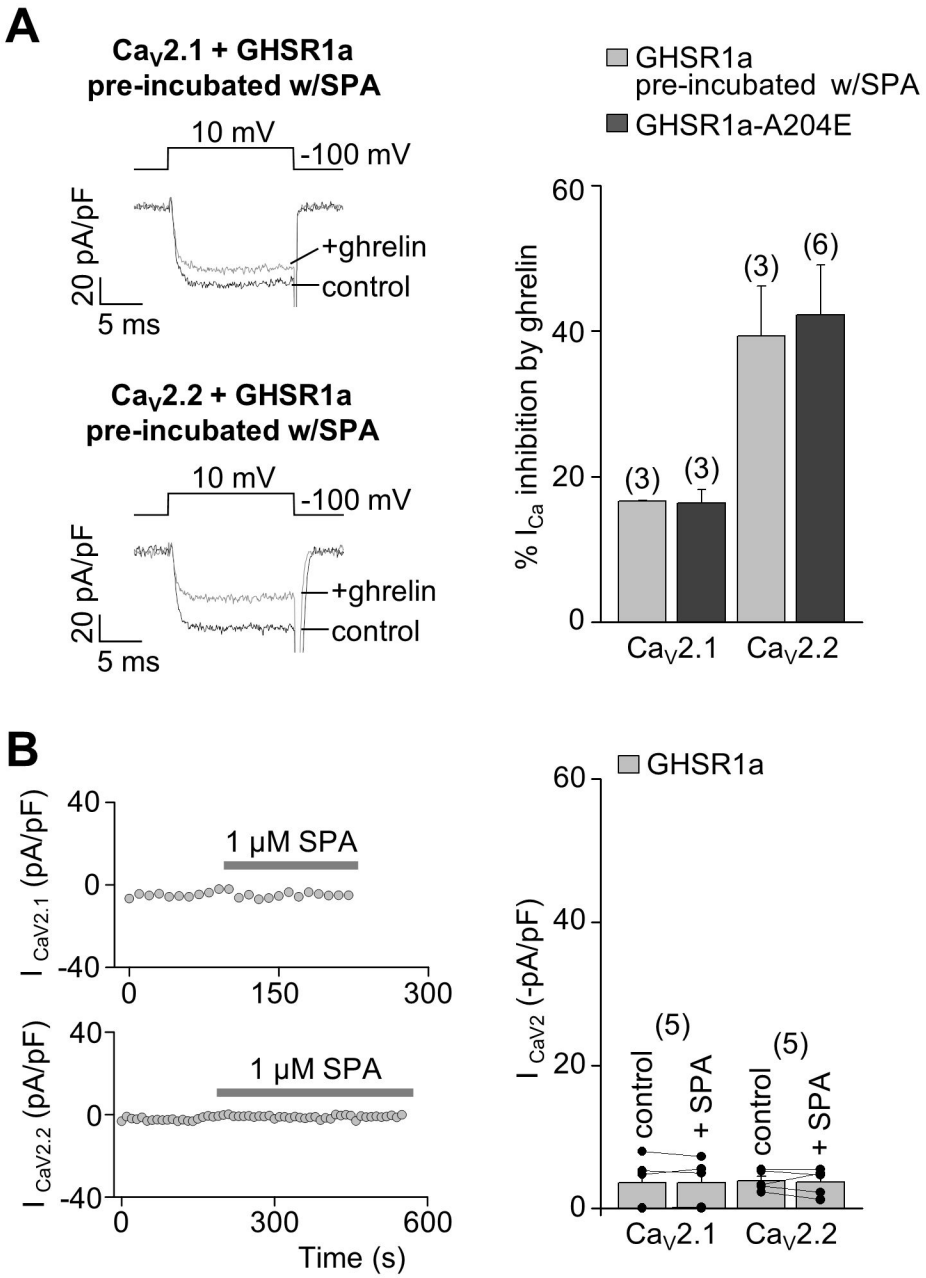
A
Ca$_V$2.1 + GHSR1a
pre-incubated w/SPA
10 mV
-100 mV
20 pA/pF
5 ms
+ghrelin
control
Ca$_V$2.2 + GHSR1a
pre-incubated w/SPA
10 mV
-100 mV
20 pA/pF
5 ms
+ghrelin
control
GHSR1a
pre-incubated w/SPA
GHSR1a-A204E
% I$_{Ca}$ inhibition by ghrelin
60
40
20
0
(3)
(3)
(3)
(6)
Ca$_V$2.1
Ca$_V$2.2
B
I $_{CaV2.1}$ (pA/pF)
40
0
-40
1 µM SPA
0
150
300
I $_{CaV2.2}$ (pA/pF)
40
0
-40
1 µM SPA
0
300
600
Time (s)
GHSR1a
I $_{CaV2}$ (-pA/pF)
60
40
20
0
(5)
control
+ SPA
(5)
control
+ SPA
Ca$_V$2.1
Ca$_V$2.2

FIGURE 2

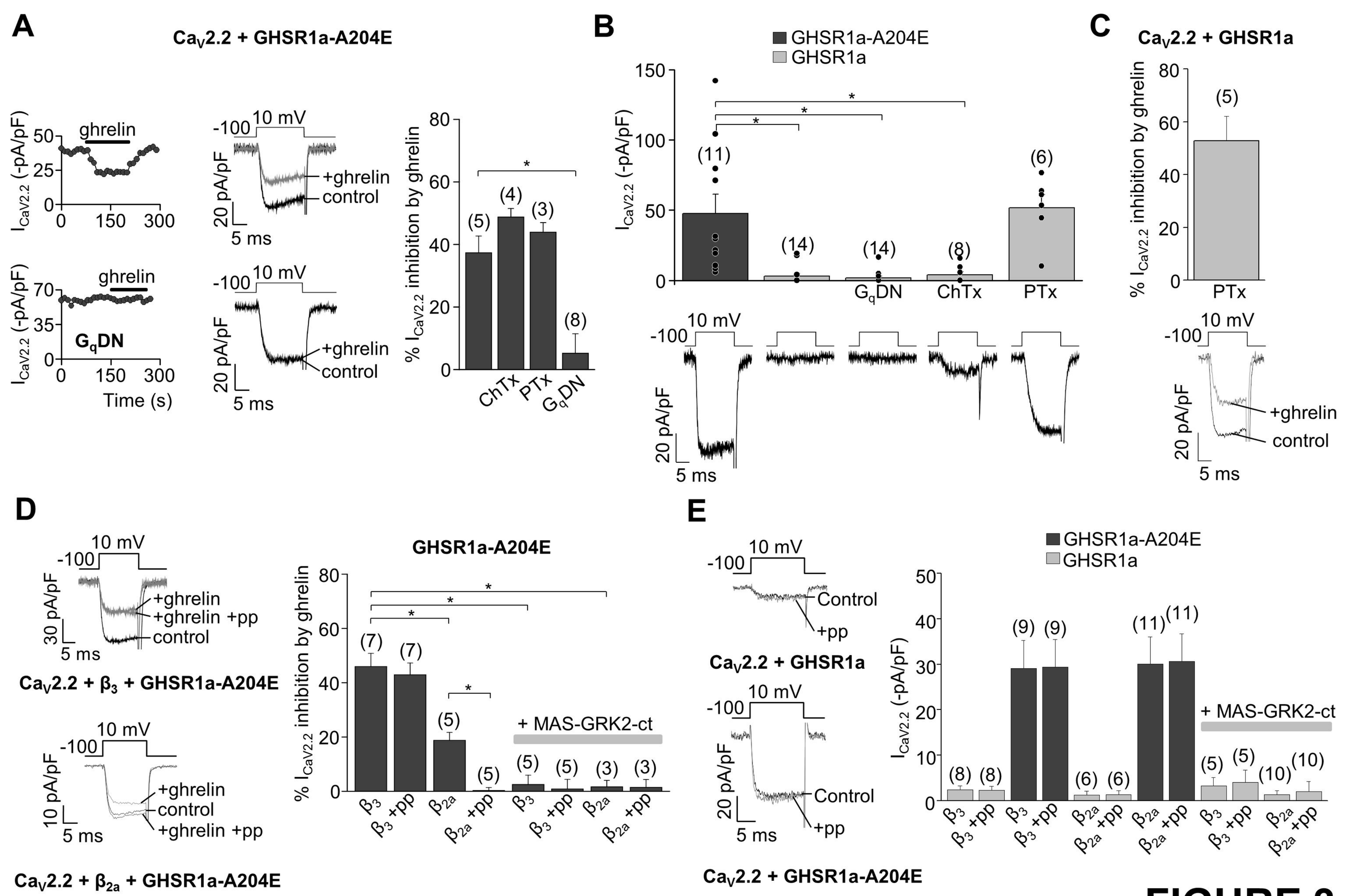
A
Cav2.2 + GHSR1a-A204E
ghrelin
ICaV2.2 (-pA/pF)
Time (s)
GqDN
-100
10 mV
20 pA/pF
5 ms
+ghrelin
control
% ICaV2.2 inhibition by ghrelin
ChTx
PTx
GqDN
B
GHSR1a-A204E
GHSR1a
(11)
(14)
(14)
(8)
(6)
C
Cav2.2 + GHSR1a
D
Cav2.2 + β3 + GHSR1a-A204E
Cav2.2 + β2a + GHSR1a-A204E
+ghrelin +pp
+ MAS-GRK2-ct
E
Control
+pp
Cav2.2 + GHSR1a
Cav2.2 + GHSR1a-A204E

FIGURE 3

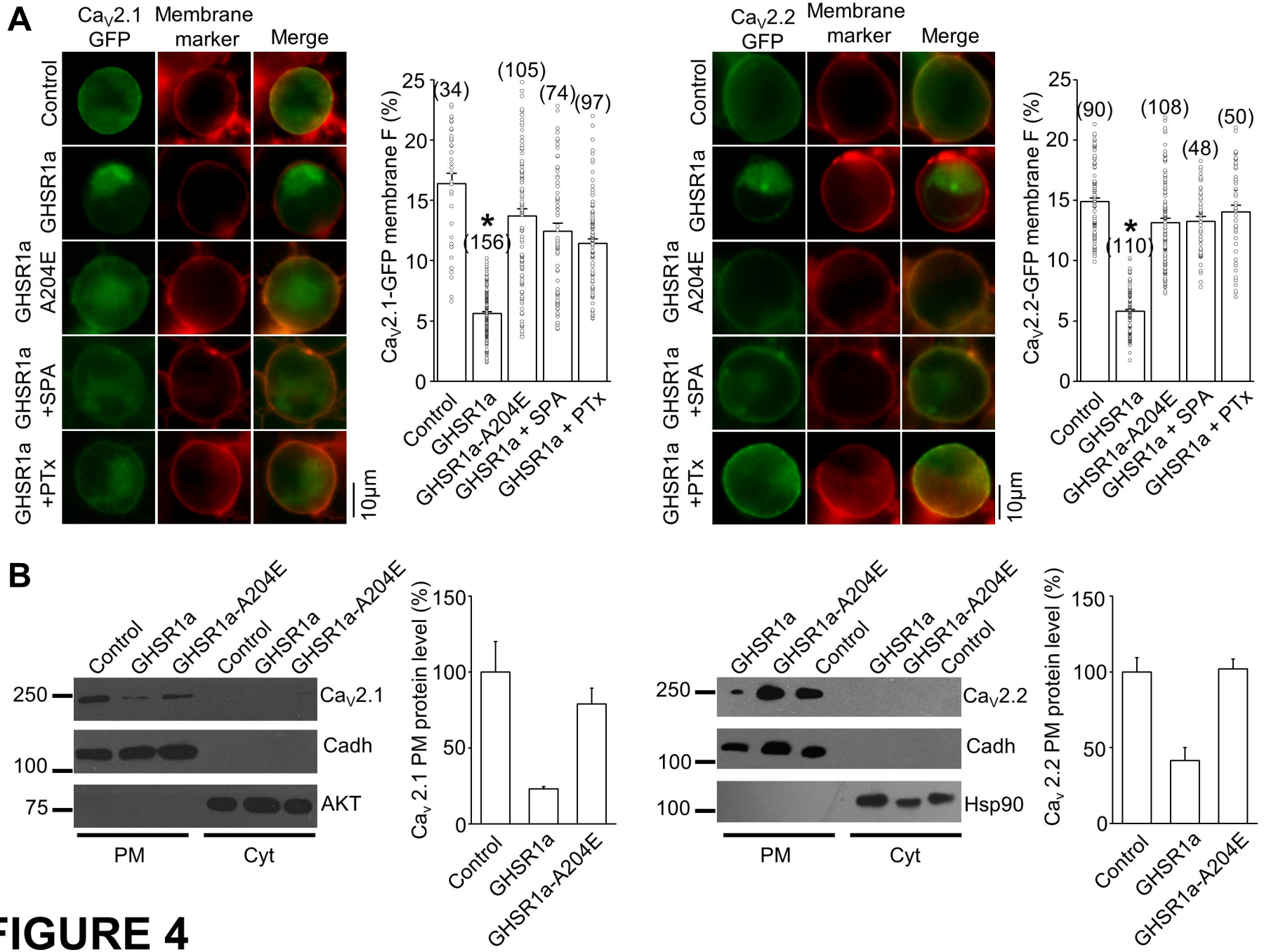
A
CaV2.1 GFP
Membrane marker
Merge
Control
GHSR1a
GHSR1a A204E
GHSR1a +SPA
GHSR1a +PTx
10μm
CaV2.1-GFP membrane F (%)
(34)
(156)
(105)
(74)
(97)
Control
GHSR1a
GHSR1a-A204E
GHSR1a + SPA
GHSR1a + PTx
CaV2.2 GFP
(90)
(110)
(108)
(48)
(50)
CaV2.2-GFP membrane F (%)
B
Control
GHSR1a
GHSR1a-A204E
250
100
75
CaV2.1
Cadh
AKT
PM
Cyt
CaV 2.1 PM protein level (%)
CaV2.2
Hsp90
CaV 2.2 PM protein level (%)

FIGURE 4

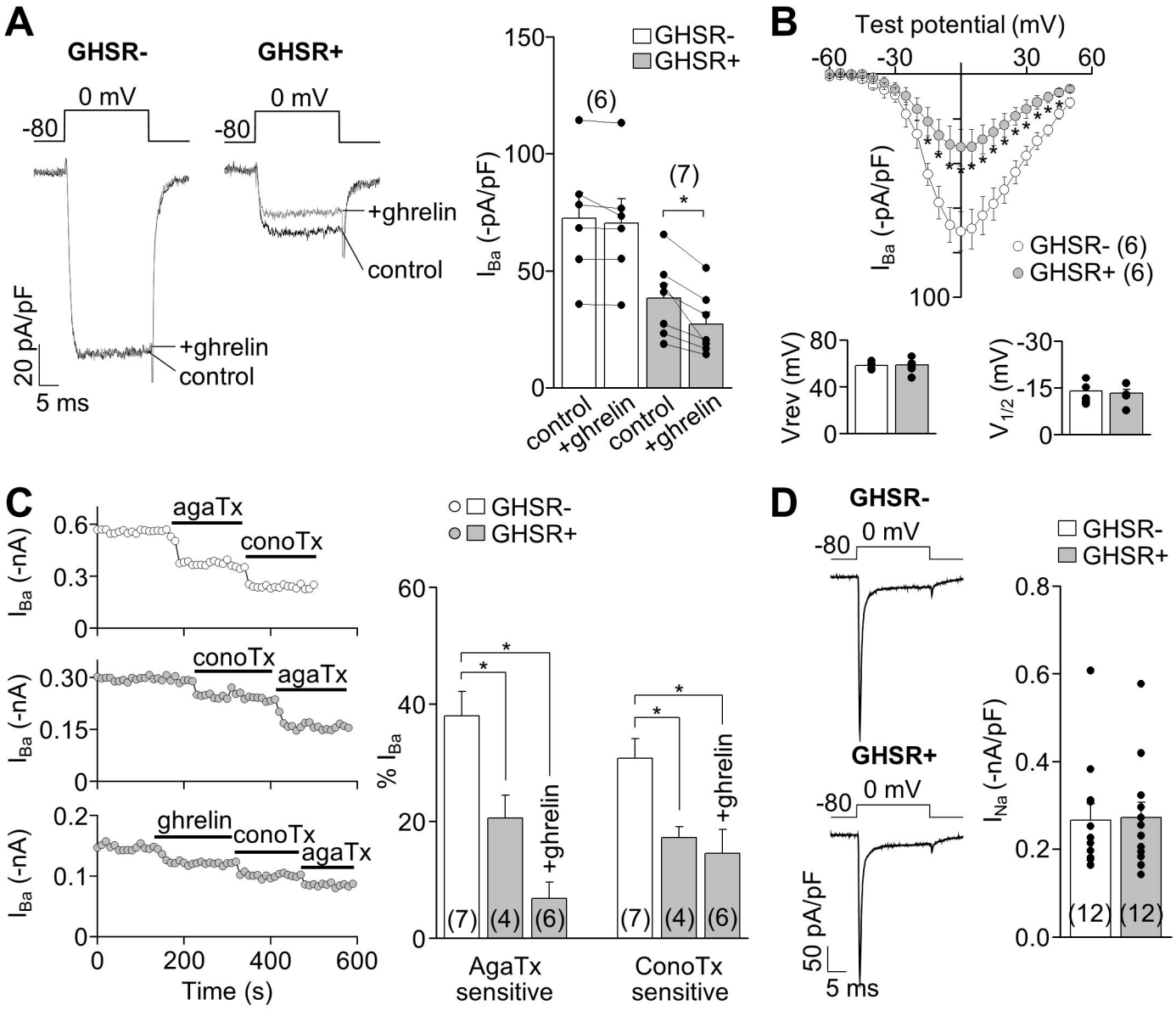
A
GHSR-
GHSR+
0 mV
-80
+ghrelin
control
20 pA/pF
5 ms
GHSR-
GHSR+
(6)
(7)
*
I_{Ba} (-pA/pF)
control
+ghrelin
B
Test potential (mV)
-60
-30
30
60
I_{Ba} (-pA/pF)
GHSR- (6)
GHSR+ (6)
Vrev (mV)
$V_{1/2}$ (mV)
C
agaTx
conoTx
ghrelin
I_{Ba} (-nA)
Time (s)
GHSR-
GHSR+
% I_{Ba}
+ghrelin
AgaTx sensitive
ConoTx sensitive
D
GHSR-
GHSR+
0 mV
-80
50 pA/pF
5 ms
I_{Na} (-nA/pF)
(12)

FIGURE 5

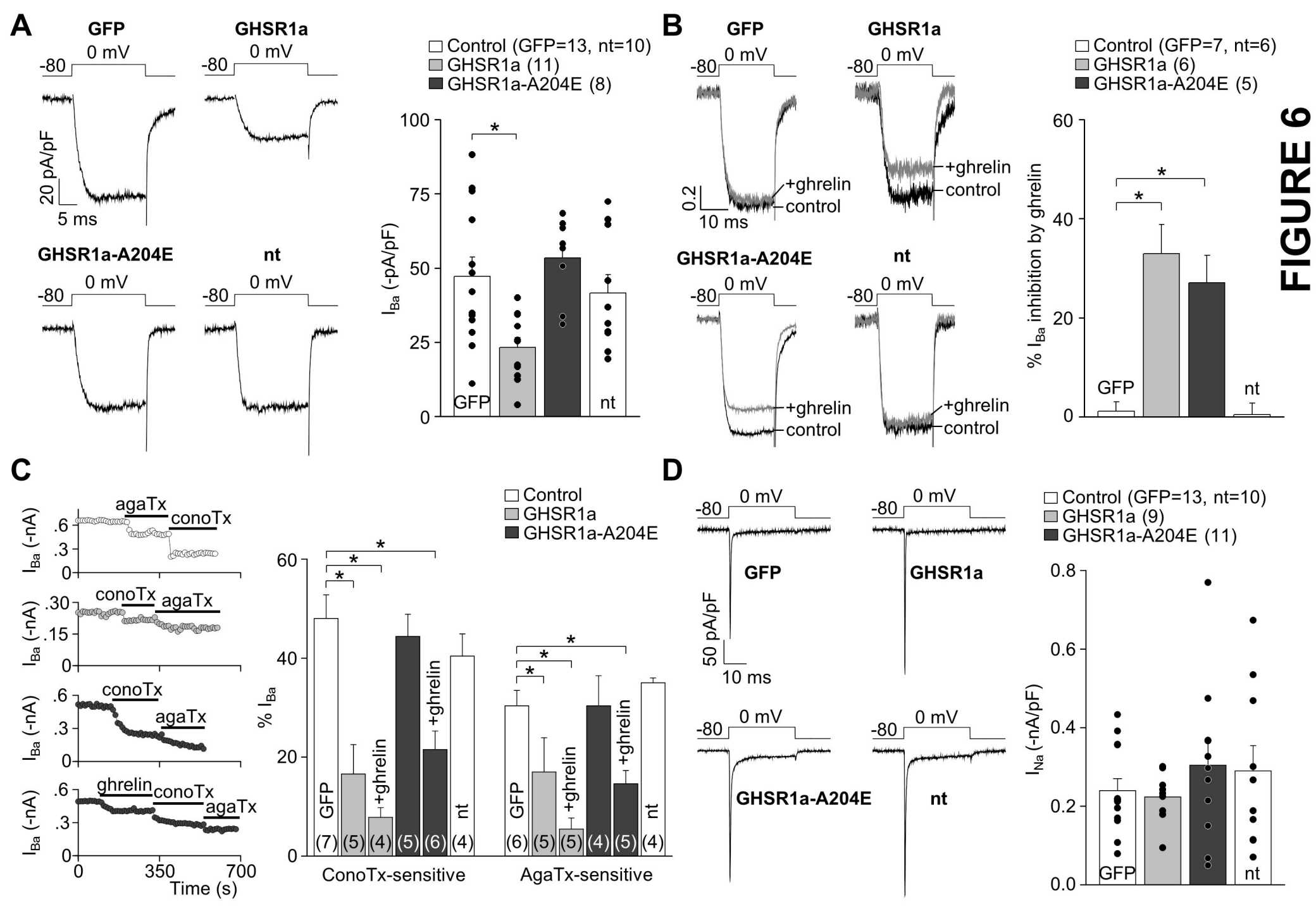
A
GFP
GHSR1a
GHSR1a-A204E
nt
0 mV
-80
20 pA/pF
5 ms
Control (GFP=13, nt=10)
GHSR1a (11)
GHSR1a-A204E (8)
I_Ba (-pA/pF)
B
Control (GFP=7, nt=6)
GHSR1a (6)
GHSR1a-A204E (5)
+ghrelin
control
0.2
10 ms
% I_Ba inhibition by ghrelin
C
agaTx
conoTx
ghrelin
I_Ba (-nA)
Time (s)
Control
GHSR1a
GHSR1a-A204E
% I_Ba
ConoTx-sensitive
AgaTx-sensitive
D
50 pA/pF
10 ms
Control (GFP=13, nt=10)
GHSR1a (9)
GHSR1a-A204E (11)
I_Na (-nA/pF)
FIGURE 6

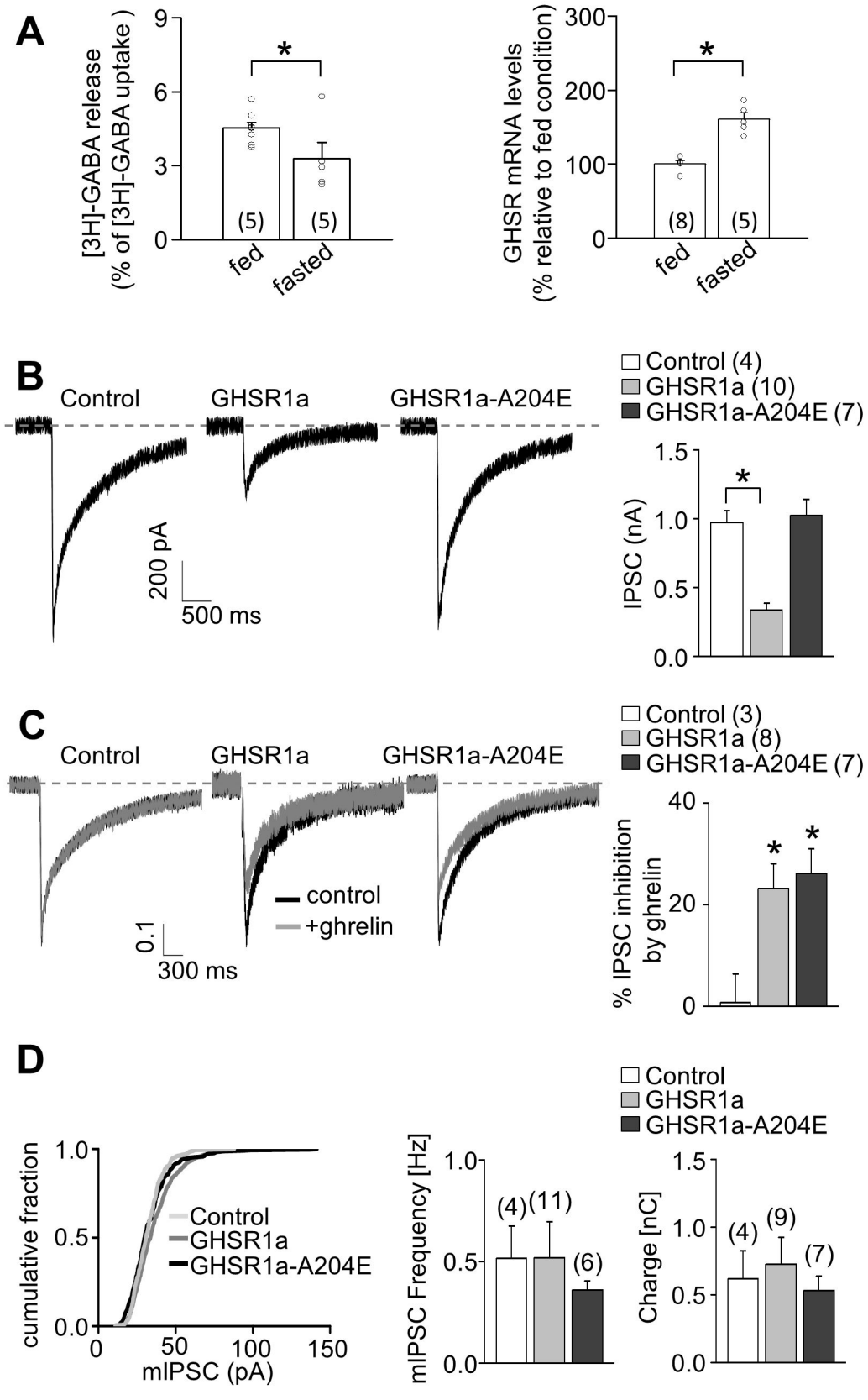
A
[3H]-GABA release
(% of [3H]-GABA uptake)
9
6
3
0
*
(5)
(5)
fed
fasted
GHSR mRNA levels
(% relative to fed condition)
300
200
100
0
*
(8)
(5)
fed
fasted
B
Control
GHSR1a
GHSR1a-A204E
200 pA
500 ms
Control (4)
GHSR1a (10)
GHSR1a-A204E (7)
IPSC (nA)
1.5
1.0
0.5
0.0
*
C
Control
GHSR1a
GHSR1a-A204E
control
+ghrelin
0.1
300 ms
Control (3)
GHSR1a (8)
GHSR1a-A204E (7)
% IPSC inhibition
by ghrelin
40
20
0
*
*
D
cumulative fraction
1.0
0.5
0.0
Control
GHSR1a
GHSR1a-A204E
0
50
100
150
mIPSC (pA)
Control
GHSR1a
GHSR1a-A204E
mIPSC Frequency [Hz]
1.0
0.5
0.0
(4)
(11)
(6)
Charge [nC]
1.5
1.0
0.5
0.0
(4)
(9)
(7)

FIGURE 7